OBJECT BASED IMAGE ANALYSIS OF GEO-EYE VHR DATA TO MODEL ABOVE GROUND CARBON STOCK IN HIMALAYAN MID-HILL FORESTS, NEPAL

NANDIN-ERDENE TSENDBAZAR
February, 2011

SUPERVISORS:
Dr. Y. Hussin
Ir. L. van Leeuwen

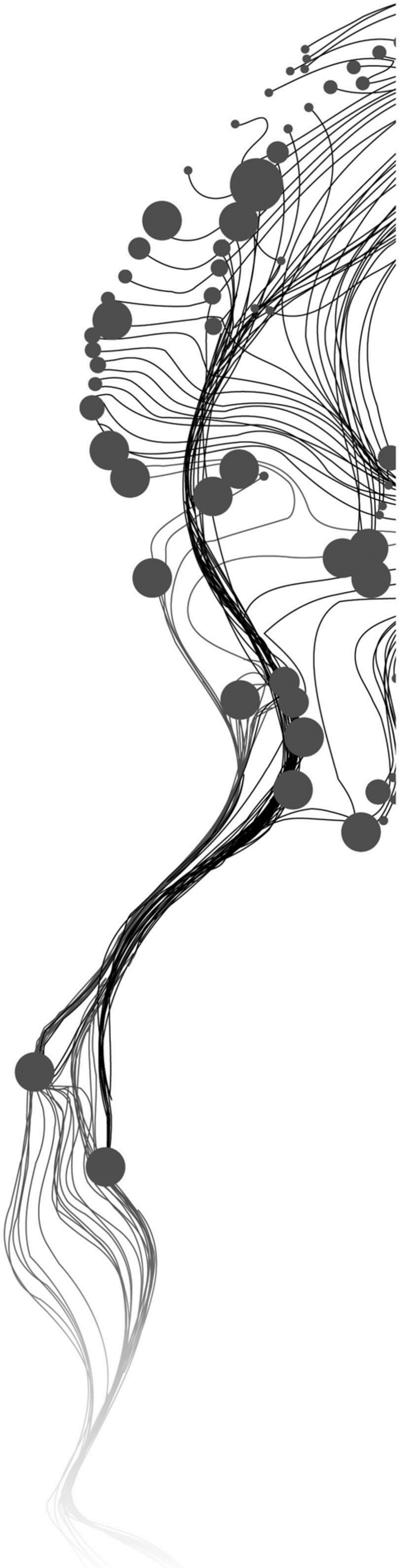

OBJECT BASED IMAGE ANALYSIS OF GEO-EYE VHR DATA TO MODEL ABOVE GROUND CARBON STOCK IN HIMALAYAN MID-HILL FORESTS, NEPAL

NANDIN-ERDENE TSENDBAZAR
Enschede, The Netherlands, February, 2011

Thesis submitted to the Faculty of Geo-Information Science and Earth Observation of the University of Twente in partial fulfilment of the requirements for the degree of Master of Science in Geo-information Science and Earth Observation.
Specialization: Natural Resources Management

SUPERVISORS:
Dr. Y. Hussin
Ir. L. van Leeuwen

THESIS ASSESSMENT BOARD:
Chair: Dr. A. Voinov
External Examiner: Prof. Dr. Thomasz Zawila-Niedzwiecki (Director, Forest Research Institute, Poland)

ABSTRACT

Recently, interest in implementing projects on reducing carbon emission from deforestation and forest degradation (REDD) for mitigating carbon dioxide emission has been increased. Consequently, an accurate and precise measurement of carbon stock in cost effective ways is needed. Fine resolution satellite imagery, together with object based image analysis (OBIA) techniques provide new opportunities to improve aboveground carbon stock estimation on the basis of allometric relationship of crown projection area (CPA) and tree biomass. This research aimed to model carbon stock in upper-subtropical forests of Nepal using very high resolution Geo-Eye imagery and OBIA.

Individual tree crown delineation approaches of Valley Following and Region Growing using 0.5 meter spatial resolution of Geo-Eye imagery were used in this research for the delineation of tree crowns in complex mixed forests. Valley Following approach was conducted in Individual Tree Crown delineation (ITC) suite in PCI-Geomatica, while Region Growing approach was done in eCognition software by developing specific rule-set. The best tree crown delineation of these approaches was further used for species and forest type classifications at individual tree crown level. Based on the field measurements of stem diameters, carbon stock of trees was calculated and the relationship between carbon stock of tree and CPA from high resolution image was analysed using simple linear regression model.

The Region Growing approach resulted in better delineation of tree crown (30% error with 75% 1:1 correspondence) than Valley following approach (40% error with 67% 1:1 correspondence). Having more accurate delineation, the delineated tree crowns from Region Growing approach were used for species and forest type classifications. Species classification resulting in 64.5% accuracy (Kappa=0.48) provided much lower accuracy than forest type classification (90.3% accuracy and Kappa=0.80). Modelling the relationship between automatically generated CPA and carbon stock of broadleaf and needle leaf trees resulted in R^2 of 0.16 and 0.34 respectively.

The results obtained in this research have agreed with previous research in tree crown delineation and species classification, while lower R^2 from modeling can be explained by rugged topography of the area, low sun elevation and off-nadir view angle of image acquisition. Nevertheless, this research indicated the utility of high resolution satellite imagery on carbon stock estimation and other forest inventories.

Key words: Aboveground carbon stock, Object based image analysis, Tree crown delineation, Region Growing, Valley Following, Crown projection area

ACKNOWLEDGEMENTS

I am sincerely grateful to the tremendous support of several organizations and people to conduct this research.

My sincere gratitude goes to the Netherlands Government and the Netherlands organisation for international cooperation in higher education (NUFFIC) for granting me a scholarship to study in the Netherlands.

I am thankful to ITC for facilitating my study and research here and my special thanks go to all NRM staff who gave me a good academic environment to learn many new skills and techniques of GIS and Remote Sensing.

I am very grateful to my first supervisor, Dr. Yousif Hussin for his unique guidance and encouragement in the successful completion of this research. I appreciate your good supervision and constructive comments. And to my second supervisor, Ir. Louise van Leeuwen, thank you for your valuable suggestions and critical comments.

A special gratitude to my course director, Dr. Michael Weir for his critical comments and suggestions during proposal defense and mid-term presentation and for his sincere guidance and concern for the welfare of all NRM students throughout the course.

I would like to acknowledge to ICIMOD project in Nepal for providing necessary data in my research and facilitating field work in Nepal. I am also thankful to FECOFUN community in Dolakha, Nepal and Krishna Khadka, Anita Khadka and Naba Raj Subedi for their kind support during field work. I would like to extend heartfelt thanks to my fieldwork mates, Srijana, Shyam, Saurav, Rachna, Rob, Sahash and Chele, who shared together the tough and cheerful moments.

To my fellow NRM students, it has been a pleasure and good experience working with a diverse group from different parts of the world and sharing different cultures and many thanks for the unforgettable time we were together.

Finally, my deepest gratitude goes to my family and friends who gave me all the strengths and supports during this whole time and for making me feel at home.

TABLE OF CONTENTS

LIST OF FIGURES

LIST OF TABLES

LIST OF ACRONYMS

AGB	Aboveground biomass
ANOVA	Analysis of Variance
CBH	Circumference at breast height
CFUG	Community forest user group
CPA	Crown projection area
DBH	Diameter at breast height
DEM	Digital Elevation Model
DN	Digital number
FSC	Forest Stewardship Counsel
GPS	Geographic Position System
HPF	High Pass Filtering
IHS	Intensity, Hue and Saturation
IPCC	The Intergovernmental Panel on Climate Change
ITC	Individual Tree Crown delineation suite
MSS	Multispectral data
OBIA	Object based image analysis
PC	Principal component
REDD	Reducing carbon emission form deforestation and forest degradation
RGB	Red, Green and Blue
UNFCCC	The United Nations Framework Convention on Climate Change
VHR	Very high resolution

1. INTRODUCTION

1.1. Background

Increase in CO_2 concentration and other greenhouse gases, have raised concerns about global warming and climate changes. The Intergovernmental Panel on Climate Change (IPCC) reported that the amount of carbon dioxide in the atmosphere is increasing by 1.4 ppm per year and this will contribute to the increase in temperature by 1.8^0C to 4^0C by the end of the century (IPCC, 2007). Dramatic increase of CO_2 concentration is highly related to human activities. Over the past 20 years, about 75% of the anthropogenic emissions of CO_2 to the atmosphere are due to fossil fuel burning (IPCC, 2001). The rest is mostly due to land use change, especially deforestation (Rohner & Staub, 2008).

Reducing carbon emissions from deforestation and forest degradation in developing countries is important to combat global warming. A tonne of carbon in trees is the result of the removal of 3.67 tonnes of carbon dioxide from the atmosphere, thus, the world's forest 'sink' holds more carbon than the atmosphere (Hunt, 2009). However, tropical deforestation is estimated to have released in the order of 1–2 billion tonnes of carbon per year during the 1990s, roughly 15–25% of annual global greenhouse gas emissions (Malhi & Grace, 2000). Thus, maintenance of existing forests as well as increasing forest area can contribute highly to the mitigation of global climate change. For this purpose, the Bali Plan Action of The United Nations Framework Convention on Climate Change (UNFCCC) in 2007 has introduced a new policy of *"Reducing emissions from deforestation and forest degradation in developing countries (REDD)"* to support the efforts to reduce emissions from deforestation and forest degradation in developing countries (UN-REDD, 2008).

Occupying 40% of its territory, Nepal's forests can be an important target for REDD project (Dhital, 2009). Nepal is a developing country where deforestation and forest degradation could influence forest fragmentation in tropical regions, consequently, it may affect Nepalese livelihoods due to their dependence on forest resources (Panta *et al.*, 2008). After facing serious deforestation issues in 1970s, forest resource is being supported to be used by community groups, as a result, over 25 % of the total forests are being managed by local communities (Dhital, 2009). Realizing forest resource importance on global carbon sequestration and livelihood of the forest community groups, Nepal submitted its interest on implementing REDD project to UNFCCC in 2008 and was granted Forest Carbon Partnership Facility for implementation of REDD project (Dahal & Banskota, 2009).

Aboveground biomass (AGB) estimation is a key for quantifying carbon stocks in forests. The carbon stored in the aboveground living biomass of trees is the largest pool and the most directly impacted by deforestation and forest degradation (Gibbs, 2007). Thus, estimation of the AGB with sufficient accuracy to analyse carbon stored in the forest is important for recently emerging policies like REDD (Basuki *et al.*, 2009). However, the most accurate method for the estimation of biomass is through cutting of trees and weighing of their parts, which is time consuming and expensive for large areas (Verwijst & Telenius, 1999). This destructive method is often used to validate other less invasive and cheaper methods, such as the estimation of carbon stock using non-destructive in-situ measurements and remote sensing (Clark *et al.*, 2001).

Remote sensing techniques, through different sensors and methods, offer a means for estimating AGB. The advantage of using remote sensing data is that spatial distribution of forest biomass can be obtained at reasonable cost and with acceptable accuracy. Examples of studies which have focused on forest biomass estimation using medium-resolution satellite imagery are *e.g.* Foody (2003) and Lu (2005). Moreover, attempts have been made to estimate forest biomass and carbon stock using different platforms (air-borne and space-borne) and sensors (optical, radar and LiDAR). However, some of these remotely sensed images tend to be inaccurate or very costly for AGB estimation in tropical forest (Gibbs, 2007). Furthermore, several methods have been proposed for estimating forest biomass using remote sensing techniques that make use of a combination of regression models, vegetation indices, and canopy reflectance models (Kajisa *et al.*, 2009). These are mainly based on pixel based approaches.

Fine resolution satellite imagery, together with object based image analysis (OBIA) techniques; provide new opportunities to improve AGB estimation analysis. OBIA and image segmentation techniques have been used in very high resolution (VHR) imagery as an option to overcome the drawbacks of conventional procedures of spectral and texture image analysis for various forestry applications (Chubey *et al.*, 2006; Morales *et al.*, 2008). For instance, Aardt *et al.* (2008), Morales *et al.* (2008) and Kajisa *et al.* (2009) have attempted to estimate AGB using OBIA and obtained reasonably good accuracy.

Relationship between stem diameter at breast height (DBH) and crown projection area (CPA) of a tree opens a possibility to calculate AGB using high resolution optical imagery where every tree is identifiable. Shimano (1997) had studied the relationship between DBH and CPA and proved that power sigmoid models can better explain this relationship than other models. Moreover, the relationship of DBH and CPA has been used to estimate aboveground carbon stock using OBIA for the delineation of CPA (Gonzalez *et al.*, 2010). Hence, using OBIA to model carbon stock in upper-subtropical forests may offer a more efficient contribution to piloting the REDD project in Nepal.

1.2. Application of remote sensing for biomass estimation

Remote sensing can offer an accurate and precise estimation of AGB and carbon stock. Estimation of AGB is the most critical step in quantifying carbon stocks from forests (Gibbs, 2007). Providing the advantages such as large access area, high correlation between spectral bands and biophysical parameters and a digital format *etc.* remote sensing based AGB estimation has been increasingly studied using different satellite imageries (Lu, 2006). A range of satellite sensors have been explored for accurate AGB estimations. Recognizing and understanding the strengths and weaknesses of different types of sensors and data is essential for selecting suitable sensors and data for AGB estimation in a specific study (Lu, 2006).

Providing up to 40 years globally consistent records, optical remote sensing has been widely used for AGB estimation (Gibbs, 2007). For instance, Landsat TM satellite imageries have been used in many applications (Lu, 2006) including AGB estimation (Baccini *et al.*, 2004; Foody*, et al.*, 2003). Moreover, spectral signatures or vegetation indices are often used for such an application. Attempts have been made to estimate forest carbon stocks indirectly by developing statistical relationships between ground measurements and satellite based vegetation indices (Foody*, et al.*, 2003; Lu, 2005). However, these methods tend to underestimate carbon stock in tropical forests where passive sensors are not effective due to dense canopy closure (Gibbs, 2007) and cause saturation in the spectral reflectance (Steininger, 2000). Furthermore, optical coarse resolution imageries are often used for biomass estimation at national, continental, and global scales (Baccini*, et al.*, 2004; Clark*, et al.*, 2001). Nevertheless, Lu (2006) reviewed that the AGB estimation based on coarse spatial resolution data is limited because of the common occurrence of mixed pixels and results in drawbacks in the integration of sample data and remote sensing derived variables.

In many areas of the world, high frequency of cloudy conditions controls the acquisition of good quality remotely sensed data by optical sensors. Thus, Radar and LiDAR imageries are used for efficiency due to its advantage of data acquisition that is irrespective of weather and light conditions (Lu, 2006). The radar backscatter returned from the ground, canopies and tops of trees are used to estimate tree height, which are then converted to forest carbon stock estimates using allometric equations (Kasischke *et al.*, 1997; Le Toan *et al.*, 2004). However, Le Toan (2004) reported that radar backscatter tends to saturate at a low biomass level, also, mountainous or hilly conditions increase errors (Gibbs, 2007). Lu (2006) reviewed an applicability of LiDAR data in forest inventory such as biomass estimation, tree height, stand volume, crown diameter and canopy structure. LiDAR images can provide AGB estimation with high accuracy since this offers information about the vertical structure of forests (Aardt*, et al.*, 2008; Ke *et al.*, 2010). Currently, nonetheless, airplane mounted LiDAR instruments are too costly to be used for small areas and a satellite based LiDAR systems could provide global coverage but is not yet an option (Gibbs, 2007).

Alternatively, the fine spatial resolution and associated multispectral (MSS) characteristics may become an important data source for AGB estimation. Many studies have been done to extract biophysical parameters using VHR images (Brandtberg, 2002; Coillie *et al.*, 2008; Culvenor, 2002; Erikson, 2004; Hay *et al.*, 2005). The spatial details of optical VHR images can be used to collect directly measurements of tree height and crown area or crown diameter. Allometric relationships between tree biophysical characteristics and CPA can be applied to estimate forest carbon stocks with high certainty (Gibbs, 2007). Gonzalez (2010) studied forest carbon densities using crown diameter estimation based on VHR Quickbird imagery and got results of high accuracy and low uncertainty. Moreover, biomass estimation based on a tree shadow fraction is also explored by Leboeuf (2007), Ozdemir (2008) and Greenberg *et al.* (2005) using VHR Quickbird imageries.

1.3. Research conceptual framework

Different methods for estimating AGB are being adopted by studies. Given the interest in implementing forestry projects for mitigating carbon dioxide emissions from deforestation and forest degradation, accurate and precise AGB and carbon stock estimations in a cost effective manner is largely demanded (Brown et al., 2005). The AGB can be directly estimated using remotely sensed data with different approaches such as multiple regression analysis, neural network and indirectly estimated from canopy parameters, such as crown diameter and crown area, which are extracted from remote sensing image (Foody*, et al.*, 2003; Lu, 2006). For example, Nath *et al.* (2009) estimated bamboo biomass using log linear model. Lu (2005) studied relationship between forest stand parameter and Landsat spectral information and vegetation indices. Many studies about biomass estimation have been done using allometry of canopy parameters (Basuki*, et al.*, 2009; Gonzalez*, et al.*, 2010; Greenberg*, et al.*, 2005; Verwijst & Telenius, 1999; Zianis & Mencuccini, 2004).

The most common mathematical model in biomass studies is based on allometry of DBH, which is highly related to other tree parameters including tree crown size (Song et al., 2010; Zianis & Mencuccini, 2004). Tree crown size is also strongly related to other parameters, such as height, biomass (Song*, et al.*, 2010). Kuuluvainen (1991) had studied the relationship between CPA, which is the vertical projection area of a tree crown on the horizontal plane, and components of biomass in Norway spruce and found a linear relationship between them. Similarly, Shimano (1997) studied relationship between DBH and CPA using different models and concluded that power sigmoid function is the most suitable one among others since growth rate of CPA slows down when DBH is sufficiently large due to competition from neighbouring trees. Moreover, Greenberg *et al.* (2005) analysed DBH and CPA derived from IKONOS imagery based on shadow allometry resulting in reasonable accuracy and then applied it to tree level biomass estimation. Thus, using CPA as an index of tree size may be useful for quantifying the carbon stock of a tree which is proportional to biomass. However, information about tree crown area is difficult to obtain and rarely available from traditional forest inventory.

CPA information can be obtained from high resolution imagery and OBIA. A significant amount of studies about delineating tree crowns based on VHR aerial photos have been done earlier due to the limitation in spatial resolution of remote sensing data from space (Song*, et al.*, 2010). Recently embedded VHR satellite based imageries such as Quickbird and IKONOS are being used to extract tree crown information successfully (Gougeon & Leckie, 2006; Hirata *et al.*, 2009; Ke*, et al.*, 2010). However, VHR imageries pose challenges because the spectral response of individual pixels does not represent the characteristics of a target entity (*e.g.* forest stand and tree crowns) since a target entity is composed of many pixels in VHR image. Thus, traditional pixel based classification using only spectral data may not work successfully with such sub-metre high resolution images since it results in a salt-and-pepper noise in the classification output (Ke*, et al.*, 2010). As an alternative to traditional approaches, OBIA was introduced and has been adapted to solve the problems related with the high spatial resolution imageries (Blaschke, 2010). It has been successfully applied to the delineation of CPA and species classification using high resolution MSS imageries (Coillie*, et al.*, 2008; Hay*, et al.*, 2005; Kim *et al.*, 2009). In contrast to pixel based classification, the basic units of OBIA are image objects (or segments) (Ke*, et al.*, 2010). Image objects are generated using an image segmentation procedure, which partitions an image into non-intersecting regions (Chubey*, et al.*, 2006). Object based classification can use not only spectral information but also other information such as shape, texture, and contextual relationships (Blaschke, 2010).

Different image segmentation techniques of OBIA are being used for forest inventory, especially for individual tree crown delineation. For instance, image segmentation for tree crown delineation can be done using Individual Tree Crown delineation suite (ITC), an extension of the image processing software PCI Geomatica (Mora *et al.*, 2010) and OBIA software eCognition (Kim*, et al.*, 2009).

ITC based Valley Following approach for tree crown delineation has been proven to be effective over a range of image types and forest conditions (Gougeon & Leckie, 2006; Leckie *et al.*, 2003). This approach of tree crown delineation is based on following the valleys of shade between tree crowns (Katoh *et al.*, 2009). The common phenomenon that on high resolution imagery, trees generally appear as bright objects surrounded by darker shaded areas is used in Valley Following approach (Gougeon, 1995). Valleys of shade or lower intensity areas between tree crowns are identified and remaining tree canopies are outlined into a crown like shapes by a rule-based system (Gougeon & Leckie, 2006; Leckie *et al.*, 2005). The delineation of deciduous trees is generally not very successful, as they may not have enough shadows or space between tree crowns (Gougeon & Leckie, 2006). As a result of Valley Following approach, researchers have obtained overall accuracies of 75% to 81% (Gougeon & Leckie, 2006; Wang *et al.*, 2004).

Moreover, Region Growing approach for tree crown delineation has been adopted by many researchers and has succeeded in delineating tree crowns (Culvenor, 2002; Erikson & Olofsson, 2005; Ke & Quackenbush, 2008). Similar to Valley Following approach, Region Growing approach assumes that the centre of the crown is brighter than the edge of the crown (Culvenor, 2002). Thus, detecting the brightest point/pixel of the crown gives a chance to locate the crown centre, and growing a region from the crown centre based on illumination image helps to delineate tree crowns (Ke & Quackenbush, 2008). Culvenor (2002) and Ke & Quackenbush (2008) have applied Region Growing approach from local maxima and resulted in up to 77% of agreement between segmented tree crowns and digitized tree crowns. Furthermore, Erikson and Olofsson (2005) compared applicability of different tree crown delineation methods such as template matching (Olofsson *et al.*, 2006), two Region Growing algorithms based on fuzzy rules (Brandtberg, 2002) and Brownian motion. Overall accuracy of around 80% for all three approaches was obtained as a result (Erikson & Olofsson, 2005).

Providing different image segmentation algorithms and advanced image object algorithms, eCognition attracts research interests on delineating individual tree crown and classifying tree species. One of the most widely used image segmentation methods for tree crown delineation is multi-resolution segmentation embedded within the commercial software eCognition. This segmentation is based on Region Growing approach starting at the level of pixel and neighbouring pixels having similar spectral values are grouped into the same objects (Platt & Schoennagel, 2009). Unlike, the Region Growing from local maxima (tree top), multi-resolution segmentation uses a user specified parameters such as the scale parameter, from which size and shape of resulting object is determined (Hay, *et al.*, 2005; Kim, *et al.*, 2009). Several studies have been done to optimize the scale parameter for individual tree crown delineation such as Kim *et al.* (2009) using spatial autocorrelation and Ke *et al.* (2010) calibrating the scale parameter. Moreover, Collie *et al.* (2008) presented automatic stand delineation method integrating wavelet analysis into the image segmentation process and proved that this method is better than traditional segmentation. Image segmentation based on eCognition can result in promising outcomes. For example, Ke *et al.* (2010) classified tree species based on multi-resolution segmentation using Quickbird and LiDAR imageries and resulted in 0.84 and 0.92 kappa accuracy respectively. Similarly, Tiede (2008) segmented individual tree crown area and succeeded 86% accurate classification for coniferous forest.

1.4. Problem Statement

Individual tree crown delineation using high resolution image is being studied by many researchers (Brandtberg & Walter, 1998; Chubey, *et al.*, 2006; Erikson, 2004; Erikson & Olofsson, 2005; Gougeon, 1995; Leckie, *et al.*, 2003). Crown delineation process has been using different approaches such as ITC based Valley Following (Gougeon, 1995), Region Growing (Ke & Quackenbush, 2008), Watershed transformation (Wang, *et al.*, 2004)), Multi-resolution segmentation (Kim, *et al.*, 2009), Wavelet segmentation (Coillie, *et al.*, 2008) and Multi-scale object specific segmentation (Hay, *et al.*, 2005). However, studies to compare these approaches, which could provide information of better tree crown delineation, have been few.

There are few studies about CPA and DBH/biomass relationship (Hirata, *et al.*, 2009; Shimano, 1997) and estimating biomass and carbon stock with this relationship using CPA from remotely sensed imagery (Gonzalez, *et al.*, 2010; Leboeuf, *et al.*, 2007). Thus, this research is devoted to address these issues.

1.5. Research objectives

The main objective of this research is to model aboveground carbon stock of upper-subtropical forests using VHR satellite images (Geo-Eye) and OBIA.

The specific objectives:

- To delineate individual tree crowns using ITC based Valley Following approach and eCognition based Region Growing approach and compare the two approaches.
- To classify tree species and forest type at a tree crown level using OBIA.
- To determine the relationship between CPA and carbon stock of trees of different species

1.6. Research Questions and Hypothesis

Objectives	Research Questions	Research Hypothesis
1.	1. What are the accuracies of tree crown delineation of ITC based approach Valley Following and eCognition based Region Growing approach? 2. Which tree crown delineation approach, Valley Following or Region Growing, is better?	**H1**: There is significant difference between accuracies of Valley Following approach and Region Growing approach on delineating tree crown.
2.	3. What are the accuracies of tree species and forest type classification?	**H1**: Accuracies of tree species and forest type classification are more than 80 %.
3.	4. How strong is the relationship between the CPA and carbon stock of tree species?	**H1**: There is a strong significant relationship between CPA and carbon stock of tree species.

1.7. Thesis outline

In Chapter 1, the conceptual framework for use of VHR satellite image and OBIA for carbon stock modelling has been introduced along with a background of application of remote sensing for biomass and carbon stock estimation. Thereafter, the research problem and research interest of this thesis have been described.

Chapter 2 will go on to briefly describe the relevant topographic, climate and vegetation characteristics of the study area.

Methods used in this research to answer research questions and achieve the research objectives are described briefly in Chapter 3. The chapter also provides information about data and materials used in this research.

Chapter 4 consists of the results of tree crown delineation approaches and its quantitative comparisons, outcomes of species classification and regression modelling.

The results are discussed in Chapter 5 and conclusions from the discussion linked to research objective and questions are drawn in Chapter 6.

2. DESCRIPTION OF THE STUDY AREA

2.1. Geographic location

The study area is situated in Charnawati watershed, located in Dolakha district of the Central Development Region, Nepal (Figure1) which is 1 of the 20 mountain districts of Nepal. It lies between 85°55' E to 86°05' E longitudes and 27°35' N to 27°45' N latitudes. The altitude ranges from 800-3500 m and the forest types span from upper tropical to sub alpine lower. This is a unique watershed having community forest user groups (CFUGs) practicing Forest Stewardship Council (FSC) Certification processes. There are 58 CFUGs within the Charnawati Watershed. The area of REDD project, which is one the main supporter of this research, is 14016 hectares out of which 5726.35 ha is forest area, 7033.37 ha is cultivation and the rest is barren land, bushes and grasslands (ANSAB, 2009).

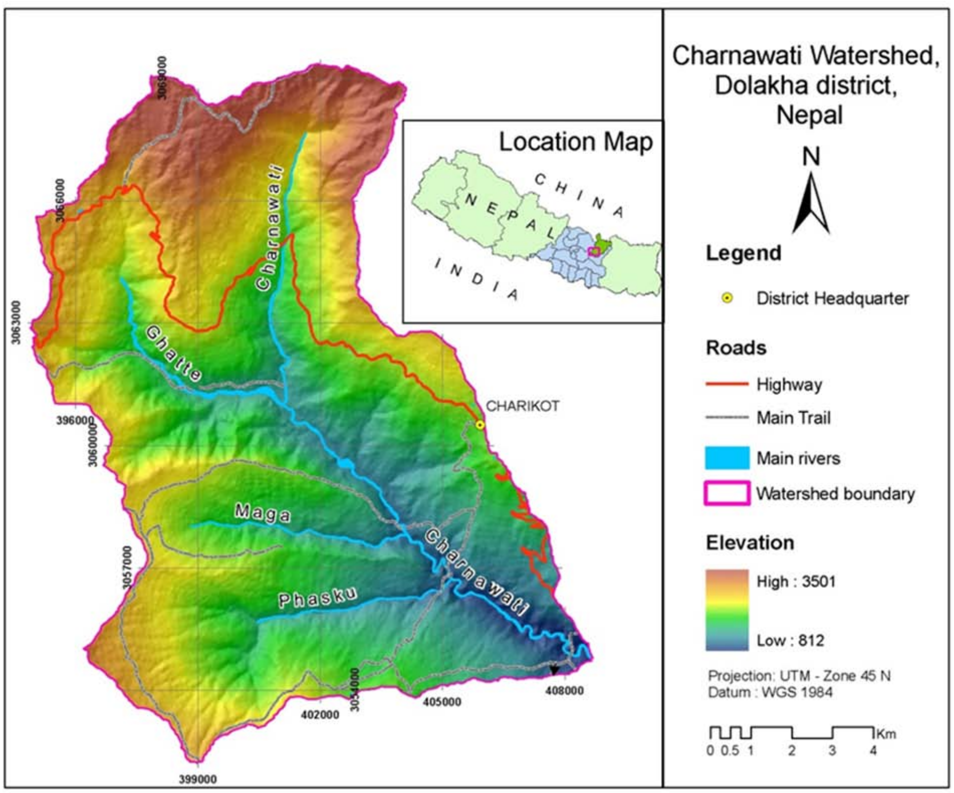

Due to the large size of Geo-Eye high resolution image of Charnawati watershed, eCognition software faced difficulty to process the whole image. Thus, a subset area of Charnawati watershed was selected for this research. The subset area is located in central eastern part of Charnawati watershed having an area of 342,9 ha consisting of 11 CFUGs areas (Figure 2). The ortho-rectified image had abnormal distorted areas in some parts and they were digitized and masked out from the subset study area.

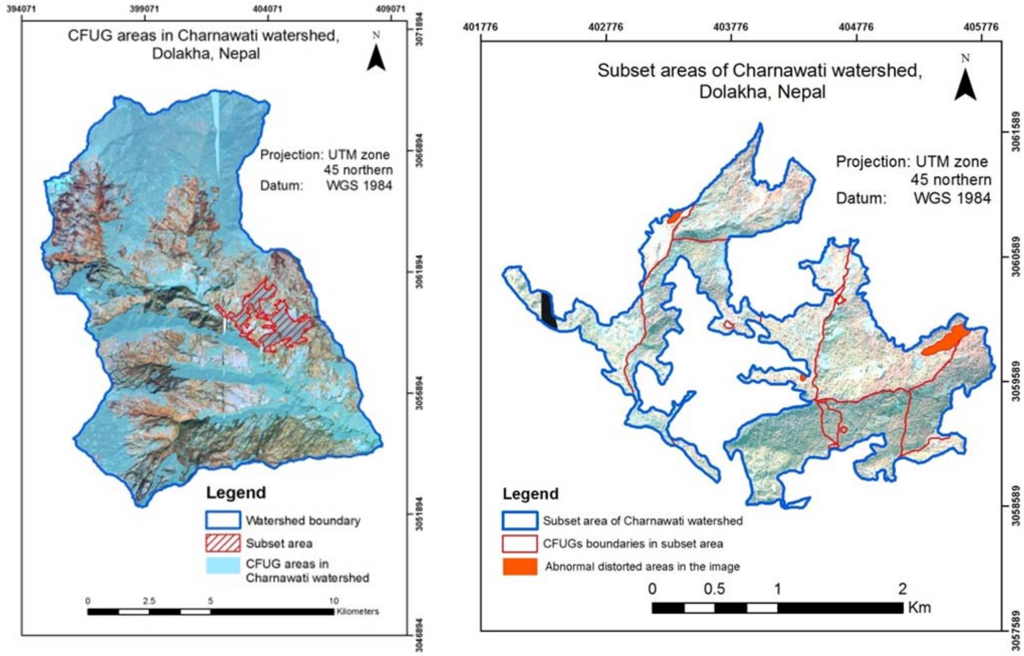

Figure 2.The subset area of Charnawati watershed

2.2. Topography

More than 61% of the Dolakha district's total area consists of land with a slope of higher than 30% (Shrestha & Dhillion, 2003). In the subset study area of Charnawati watershed, elevation ranges from 1200m to 2000m and up to more than 50^0 steep slopes can be found (Figure 3). In the south-western side, it connects to river valleys. Moreover, south, south-west, west, north-west, and northern aspects are the most dominant aspects in this area (Figure 4).

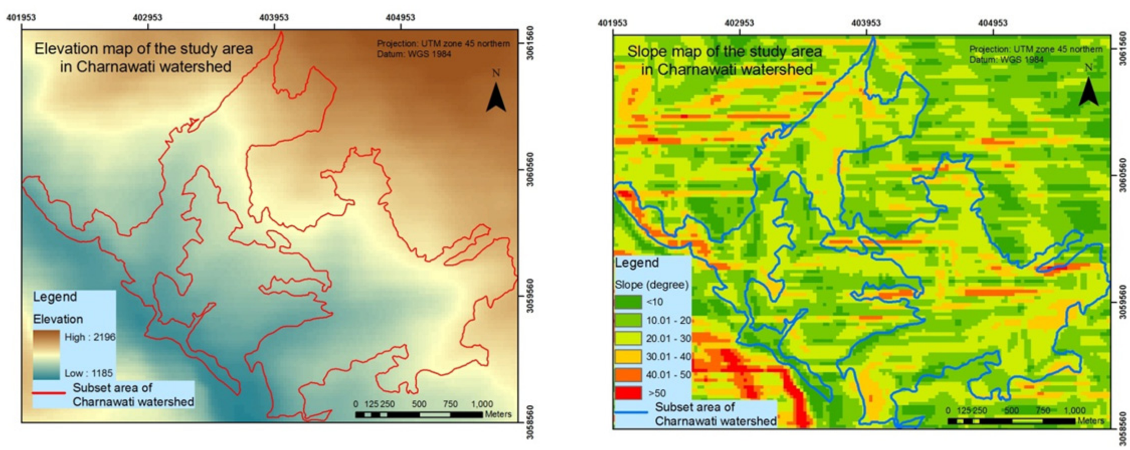

Figure 3. Elevation and slope map of the subset study area in Charnawati watershed

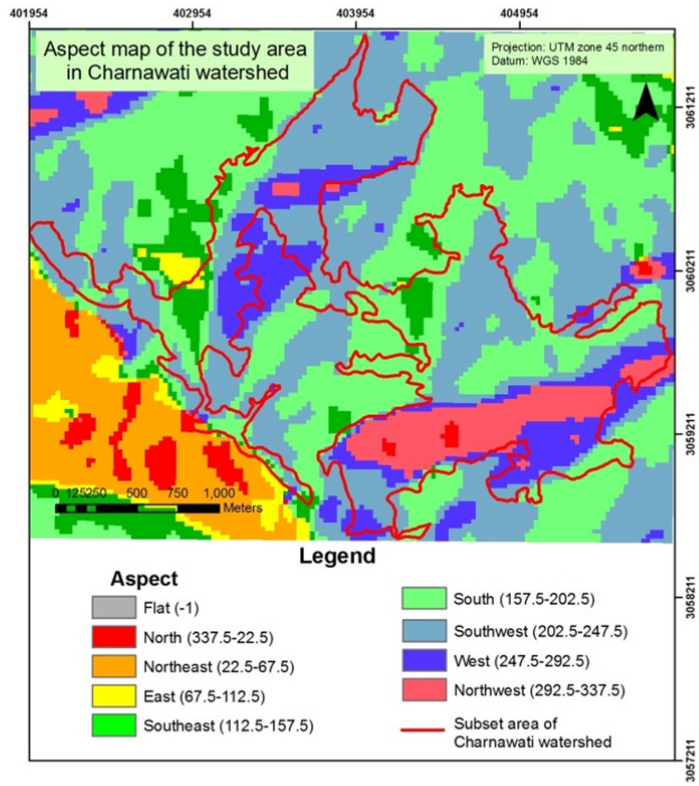

Figure 4. Aspect map of the subset study area in Charnawati watershed

2.3. Climate

Dolakha district is ranged from sub-tropical to alpine climate. Average rainfall of the district is 2044 mm and the maximum temperature recorded in the district is 35 °C and the minimum is 8°C (Shrestha & Dhillion, 2003). The monsoon season ranges from June to September, and it accounts for about 80% of the total annual rainfall (Shrestha & Dhillion, 2003). 50 year average (1950-2000) monthly air temperature and monthly precipitation of Charikot, Dolakha are shown Figure 5 (Hijmans *et al.*, 2005).

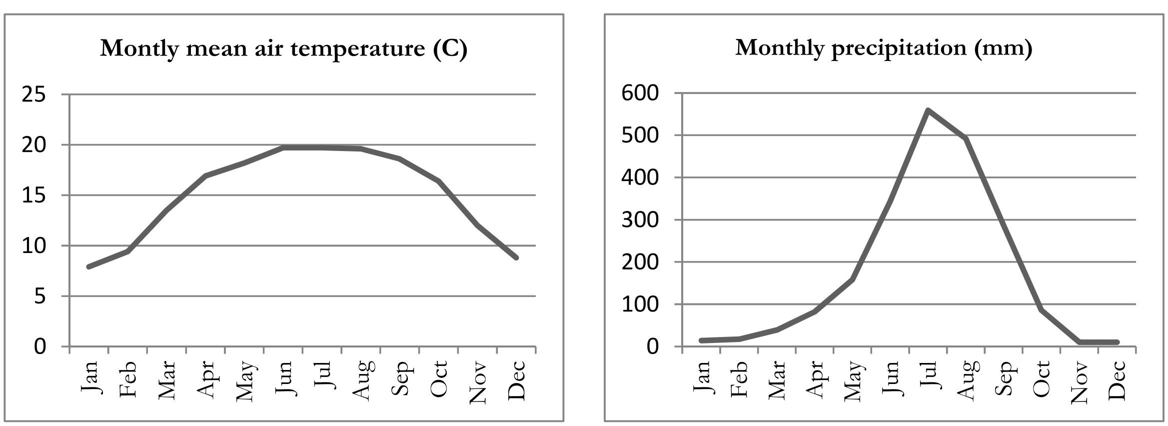

Figure 5. Monthly mean air temperature and monthly precipitation of Charikot, Dolakha, Nepal

2.4. Vegetation cover

Vegetation ranges from hardwood forests in the low land through coniferous and mixed broad-leaved forests at the mid to upper elevations and high altitude coniferous forest to alpine conditions above the tree line, which lies at about 4000 m (ANSAB, 2009). For needle leaved forests, *Pinus roxburghii, Pinus wallichiana* and *Pinus patula* are the most common species, while; *Alnus nepalensis, Schima wallichiana*, and *Quercus semecarpifolia* are the dominant species in broad leaved forests. Moreover, R*odhodendron* families having slow growth rate such as *R. arboretum, R campanulatum, and Lyonia ovalifolia* are common in upper temperate regions (Shrestha & Dhillion, 2003).

In the subset study area of Charnawati watershed, upper-subtropical forest is dominant. *Pinus roxburghii, Alnus nepalensis*, and *Schima wallichiana* are the most common species and they occur in 1000-2000 m elevation (Bajracharya, 2010; Mohns, 1988).

3. DESCRIPTION OF METHOD AND DATA USED

3.1. Material description

3.1.1. Data set

Geo-Eye1 data

Geo-Eye1 satellite was launched by Geo Eye on 6th September 2008 in the U.S. Geo-Eye1 has the highest resolution of any commercial imaging system and can collect images with a ground resolution of 0.41 meters in the panchromatic and it collects MSS at 1.65 meter resolution. However, the satellite collects imagery at 0.41 meters, Geo-Eye's operating license from the U.S. Government requires re-sampling the imagery to 0.5 meter for all customers who are not explicitly granted a waiver by the U.S. Government.

In this research, Geo-Eye1 imagery that has an acquisition date of 2nd November 2009 was used and the image specifications are shown in Table 1. Ortho-rectification was done by ICIMOD project in Nepal.

Table 1**. Satellite image characteristics**

Sensor name	**Geo-Eye1**
Spatial resolution	Panchromatic : 0.5 m Multispectral: 2 m
Dynamic range	11 bits
Band Wavelength (μm)	Blue 0,45- 0,51 Green 0,51- 0,58 Red 0,655 - 0,69 NIR 0,78 - 0,92 PAN 0,45 -0,8
Orbit height	684 kilo meters
Orbit type	Sun-synchronous
Swath width	15.2 km
Processing Level	Geometrically and Radiometrical correction
Projection	Universal Transverse Mercator UTM Specific Parameters Hemisphere: N Zone Number: 45
Datum	WGS84
Nominal collection azimuth	315.3 degree
Nominal collection elevation	64.6 degree
Sun angle azimuth	163,5 degree
Sun angle elevation	46.0 degree
Acquisition time	05:12 GMT; 10:57 Katmandu

Other reference dataset

Other reference data provided by ICIMOD were used in this research, including:

- Topographic Maps at 1:25000 scale (Source: Survey Department of Government of Nepal, 2786-05A, 2786-05C, 2785-08B and 2785-08D)
- Digital Elevation Model (DEM) 20 m resolution (generated from contour lines of topographic maps)
- Dolakha geo-database, which consists of land cover, CFUG areas, road, rivers, village centres *etc.* (digitized from topographical maps with 1:25000 scale)

3.1.2. Other materials

In addition to the dataset, other materials were used including:

- Instruments used in the field work (Table 2)
- Software required for data analysis and thesis writing (Table 3).

Table 2**. List of instruments used for field work**

Instruments	***Purpose of usage***
iPAQ and GPS	Navigation
Suunto compass	Orientation
Diameter tape 5 meters	Diameter measurement
Measuring tape 30 meters	Length measurement
Spherical densiometer	Crown cover measurement
Slope meter	Slope measurement
Haga altimeter	Tree height measurement
Fieldwork datasheet	Field data record

Table 3**. List of software used in this reserach**

Software	***Purpose of usage***
ArcGIS 10	GIS analysing
Erdas Imagine 10 ENVI 4.7.2.	Image processing
eCognition 8	Tree crown delineation and classification
ITC, PCI-Geomatica	
R software	Statistical analysis
SPSS	
Adobe Acrobat Professional	Thesis writing and editing
Microsoft Office End note	

3.2. Methods

MSS and panchromatic image of Geo-Eye were fused to create pan-sharpened MSS image and this pan-sharpened image was smoothed by applying median filters to remove the noise of high resolution image. Individual tree crown delineation was done based on two approaches namely Region Growing using eCognition software and Valley Following using ITC suite in PCI-Geomatica. Using delineated tree crowns as objects, tree species classification was conducted based on the spectral information of pan-sharpened MSS image. Area of delineated tree crowns was calculated and used as an explanatory variable to predict the amount of carbon stock per tree. The method to carry out this research is described in the flowchart of Figure 6. Detailed explanation is described in the following subsections.

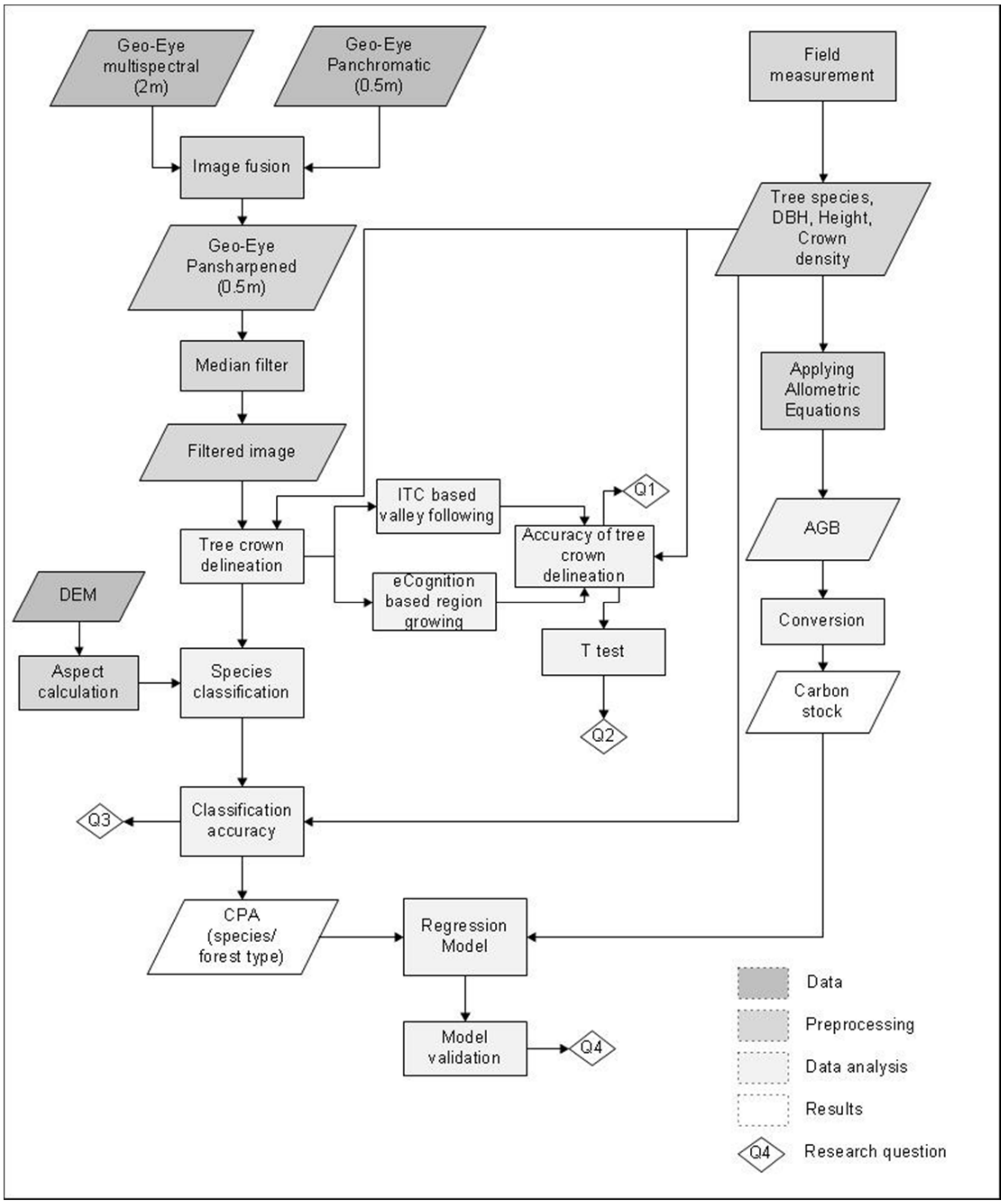

Figure 6. Flowchart of research method

3.2.1. Image fusion

Image fusion is a technique to enhance MSS images with high radiometric resolution geometrically by merging it with a panchromatic image (Neteler & Mitasova, 2008). Several image fusion methods like Intensity, Hue and Saturation (IHS), principal components (PC), and watershed transformations are commonly used for image processing.

The IHS fusion method can effectively separate RGB (red, green, blue) image into spatial (I) and spectral (H, S) information. Intensity (I) refers to the total colour brightness. Hue (H) refers to the dominant or average wavelength contributing to a colour and saturation (S) refers to the purity of a colour relative to grey (Junli *et al.*, 2005). The general idea of IHS fusion is to replace the intensity channel with a high resolution panchromatic image for the back-transformation from the IHS to RGB colour model (Neteler & Mitasova, 2008). As a result, the spectral information in lower resolution is merged with the high spatial resolution of the panchromatic image.

The principle of PC fusion is similar to that of IHS method since PC1 of MSS image is replaced by panchromatic data before the image is transformed back to the original image space (Pande *et al.*, 2009). The main advantage of this fusion is that more than three bands can be used for image analysis after the fusion process. Similarly, High Pass Filtering (HPF) based resolution-merge algorithm merges different resolution images and creates a fine spatial and spectral resolution image containing 3 or more bands. HPF resolution-merge algorithm introduces HPF to high spatial resolution image in order to get high frequency information that is mostly related to spatial information (Chavez *et al.*, 1991). Then, HPF results are added, pixel by pixel, to lower spatial resolution and higher spectral resolution data set. This allows us not to distort the spectral balance of MSS image and gives very close spectral information to that of original MSS image (Ahmad & Singh, 2002). This HPF resolution-merge algorithm has been proven to be useful in a spectral analysis, specially spectral classifications (Ahmad & Singh, 2002).

HPF resolution-merge fusion process was carried out using Geo-Eye MSS image (2 m spatial resolution) and Geo-Eye panchromatic image (0.5m spatial resolution). As a result, a MSS pan-sharpened image that has 0.5 meter resolution was created for further image analysis.

3.2.2. Low pass (median) filter

Image processing technique called filtering is used to enhance images. Filtering techniques can be divided into two main types such as low pass filters and high pass filters (Clark & Rilee, 2010). Low pass filters are used to remove small random spatial variations, typically noise, through averaging or smoothing process (Neteler & Mitasova, 2004). Noise will be removed, but some high frequency signal as well. On the other hand, a series of high pass filters with carefully selected thresholds can be used to detect edges or shapes on the image (Clark & Rilee, 2010).

Prior to segmentation, a median filter is applied to avoid over-segmentation (Platt & Schoennagel, 2009). A median filter is used since it produces more homogeneous image segments and may reduce the amount of convolutions in the final segmented polygons as a consequence of the VHR images (Mora*, et al.*, 2010). Depending on homogeneity of the images, researchers have used different window sized median filters for individual tree crown delineation, but window size of 3-by-3, 5-by-5, and 7-by-7 are the most commonly used (Erikson & Olofsson, 2005; Gougeon & Leckie, 2006; Mora*, et al.*, 2010; Platt & Schoennagel, 2009). In this study, 3-by-3 and 5-by-5 median filters were used.

3.2.3. Tree crown delineation

OBIA takes groups of pixels or "objects" instead of individual pixels as the unit of classification (Chubey*, et al.*, 2006). Each object is composed of spatially adjacent pixels based on homogeneity criteria (Ke*, et al.*, 2010). Image segmentation procedures are used to generate image objects by partitioning an image into non intersecting regions (Blaschke, 2010). Similarly, for the delineation of individual tree crowns, OBIA is used to create objects that roughly approximated the size and shape of the individual tree crown area (Kim*, et al.*, 2009).

Tree crown delineation using Region Growing approach in eCognition

eCognition provides several different approaches of segmentation, ranging from very simple algorithms, such as chessboard and quad-tree segmentation, to highly sophisticated methods such as multi-resolution segmentation and contrast filter segmentation (Definiens 2009). Moreover, this software provides advanced image classification algorithms such as finding local maxima and minima, and advanced object reshaping algorithms namely 'grow region' and 'morphology' *etc.* (Definiens 2009). These algorithms also can be applied to tree crown delineation.

One of the most commonly used image segmentation methods is the multi-resolution. This is a bottom-up region growing algorithm, which starts with one pixel objects and subsequently merges pairs of adjacent objects into larger objects based on the smallest growth of heterogeneity, which is defined through both spectral variance and geometry of the object (Definiens 2009). Region growing also can be done using specified seed points using rule based algorithms in eCognition.

Starting at potential seed pixels, neighbouring pixels are examined sequentially and added to the growing region if they are sufficiently similar to the seed pixels (Ke & Quackenbush, 2008). In the studies of tree crown delineation, local maxima are used to provide position of each seed. In VHR illumination images, it is assumed that the centre of a crown is brighter than the edge of the crown (Culvenor, 2002; Ke & Quackenbush, 2008). At the scale of individual tree crowns, crown peaks correspond brighter in the image because of higher level solar illumination (Culvenor, 2002). Moreover, a radiometric tree crown profile derived from remotely sensed imagery may be considered similar in shape to the geometrical profile of it, thus high resolution remote sensing image provides a useful clue for automatic tree top detection.

The three dimensional analogy is useful for describing this principle in tree crown delineation process. The spatial information in the image is represented in x and y dimension, while brightness value of the image is shown in vertical (z) axis, which results in a radiometric topography of individual tree (Figure 7) (Culvenor, 2002). Local maxima in an illumination image are assumed as tree tops and can be seen as the pick of a mountain in radiometric topography of individual trees. On the other hands, local minima are assumed to be shadow or space between tree crowns, thus seems as valleys in radiometric topography.

In Region Growing approach, local radiometric maxima are used as seeds for growing and local minima are used as a restriction for growing region (Culvenor, 2002).

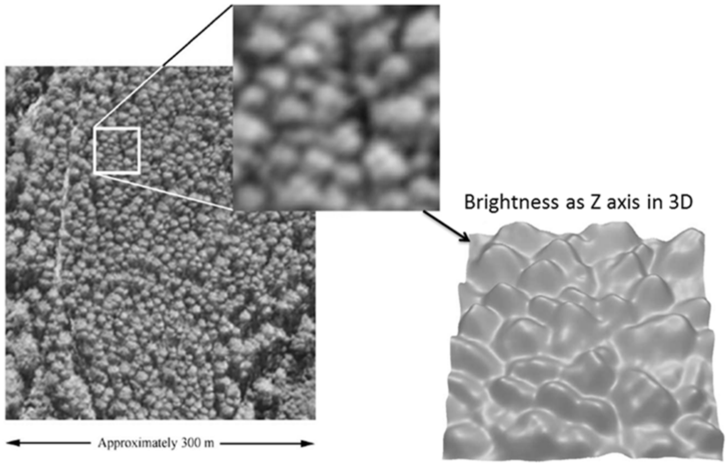

Figure 7. Radiometric 'topography' of subset of VHR imagery (Culvenor, 2002)

Tree crown delineation using Region Growing approach in eCognition was based on panchromatic image. To increase the processing time of eCognition, large shadow areas were masked in Erdas Imagine and imported to eCognition. Areas that have less than 460 DN values were masked out.

Tree crown delineation using eCognition has been done with following three main steps:

a. Delineation of valleys between trees using local minima and growing from it
b. Delineation of tree crowns based on tree top detection using local maxima and growing from it
c. Refining the shape of tree crowns.

a. Delineation of valleys between trees using local minima and growing from it

The purpose of delineating valleys is to prevent the region growing of tree crowns to be too big, especially in dense forest areas. To find the valleys (shadow) between trees, chessboard segmentation was used to create identical sized objects and 2X2 pixel sized objects found to be appropriate based on processing capability of eCognition. Using these objects, local minima with search range of 3 objects (6 pixels) was calculated. Moreover, Conditional Quad Tree segmentation (eCognition Community, 2008) was applied to the objects neighbouring to local minima to create objects of one pixel size. Local minima seeds (objects) were grown with respect to neighbouring objects that have the least mean difference to the darker objects in panchromatic image. Darker objects, here, are assumed to be local minima. Thus, objects that have the least difference to local minima were merged and grown to delineate valleys between trees. False valleys were found in dense forest areas and they were classified as trees. Steps related to delineating shadow areas between tree crowns and its corresponding rule-set are shown in Figure 8.

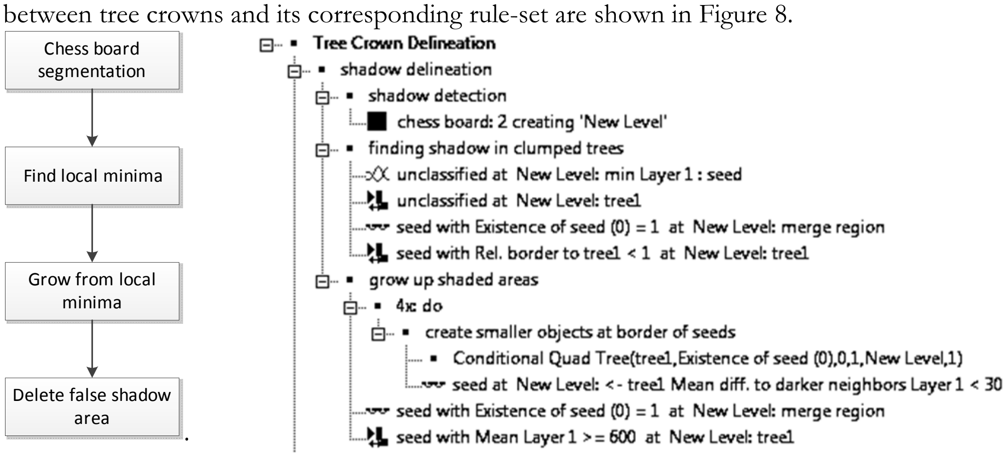

Figure 8. Steps related to delineating valleys (shadow areas) and its corresponding rule-set

b. *Delineation of tree crowns based on tree top detection using local maxima and growing from it*

Image objects except valleys between trees were segmented again using Chessboard segmentation to create identical sized (2 by 2 pixels) objects since false valleys from valley delineation were merged with tree objects. Afterwards, local maxima (tree tops) were detected with search range of 5 objects (to detect smaller tree crown recorded in the field). Conditional Quad Tree segmentation (eCognition Community, 2008) was also applied to the neighbouring objects of local maxima to create objects of one pixel size. Neighbouring objects to tree top were examined in terms of their similarities using parameter of mean difference to brighter neighbours and added to the growing region if they are sufficiently similar to the seed object. To remove false local maxima (tree top), grown tree tops which neighbours to one another were merged in first two steps of region growing. Region growing from tree tops was continued until significant boundaries of tree crowns found. Growing region was stopped based on visual examination. Figure 9 shows the steps of tree crown delineation and its corresponding rule-set.

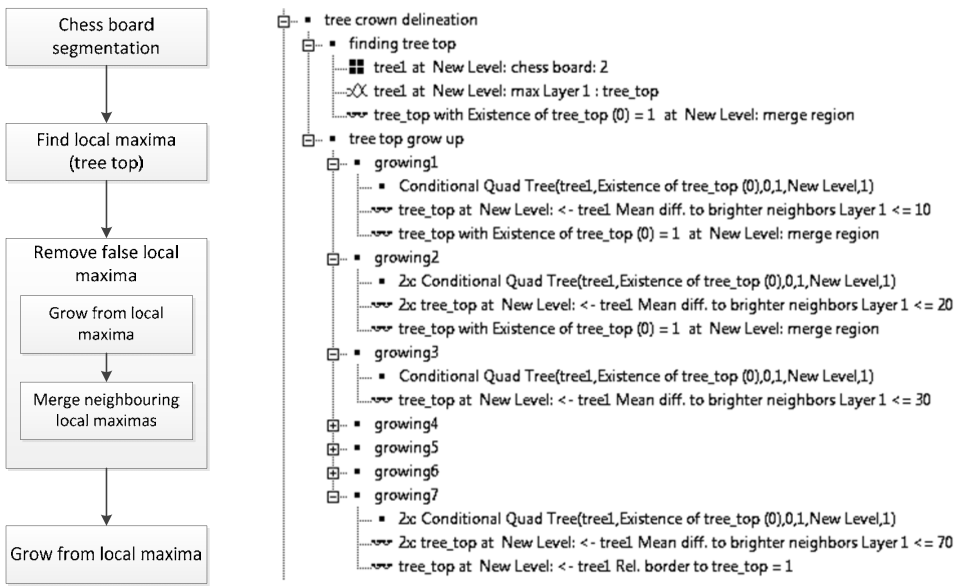

Figure 9. Tree crown delineation steps and it's corresponding rule-set

c. *Refining the shape of tree crowns*

After growing regions from tree tops, the shape of the tree crown was smoothed using 'morphology' algorithm. Moreover, tree crowns that cover a smaller area than 6 pixels were identified as non-tree to remove noise from crown delineation. In addition, some temporary classes except tree crowns were merged to shadow class. Steps followed to refine the shape of tree crowns are presented in Figure 10.

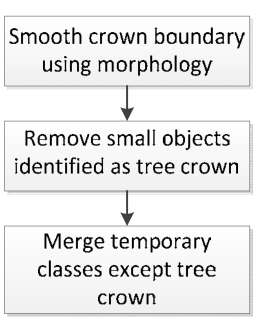

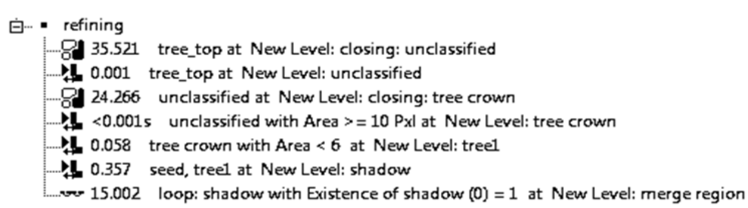

Figure 10. Steps followed to refine the shape of tree crowns and its corresponding rule-set.

Tree crown delineation using ITC based Valley Following approach

ITC software uses "Valley Following" approach, which is based on a premise that there are high intensity values on tree crowns and low intensity shaded pixels between crowns, thus forming peaks of brightness and valleys of lower intensity on the imagery (Leckie*, et al.*, 2005). This algorithm was originally developed by Gougeon (1995) for automated delineation of trees in a mature coniferous forest stand in Canada.

This approach first finds local minima in an illumination image and follows all possible valleys of shade in the image pixel-by-pixel until the valley ends or reaches a specified maximum illumination value (Gougeon & Leckie, 2006). This results in a preliminary separation of potential tree crowns. In Valley Following process several parameters should be specified by the user.

- Lower threshold: to eliminate small areas of shade
- Upper threshold: to limit valley progression into high radiance values for preventing crowns from being over-broken
- A valley noise to compensate for radiometric noise.

The Valley Following process is followed by a rule-based crown delineation process, which follows the crown boundaries favouring clockwise motions trying to close the loop to end at the starting pixel (Katoh*, et al.*, 2009). Higher-level rules identify small indentations in the potential crown boundary and permit the boundary to jump across the indentation if there are other valley pixels within a specified direction and distance (jump factor) from the indentation (Leckie*, et al.*, 2005). As a result, individual objects representing possible tree crowns are outlined. These are referred to as isols (Gougeon, 1995). Prior to the process of individual tree crown delineation, masking out non forest areas is advised (Figure 11).

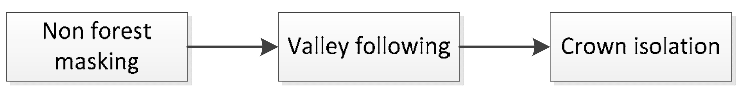

Figure 11. Processes related to individual tree crown delineation using Valley Following approach

In this research, non-forest areas were masked using pan sharpened MSS image in ITC suite. Valleys between tree crowns were delineated using smoothed pan-chromatic image with kernel size of 5 by 5 pixels and default lower threshold 358, upper threshold 774, valley noise 2. Different combinations of these parameters were checked but did not make a significant improvement on delineated valleys. Moreover, "mature" tree jump factor option was used for isolating tree crowns, since it works better for big tree crowns.

Basic concepts of these two tree crown delineation approaches are shown in Figure 12. Both the approaches are based on the same concept of radiometric topography of trees in VHR image (Figure 7.) Difference of these two approaches is that Region Growing uses local maxima and local minima, while Valley Following approach uses local minima for tree crown delineation.

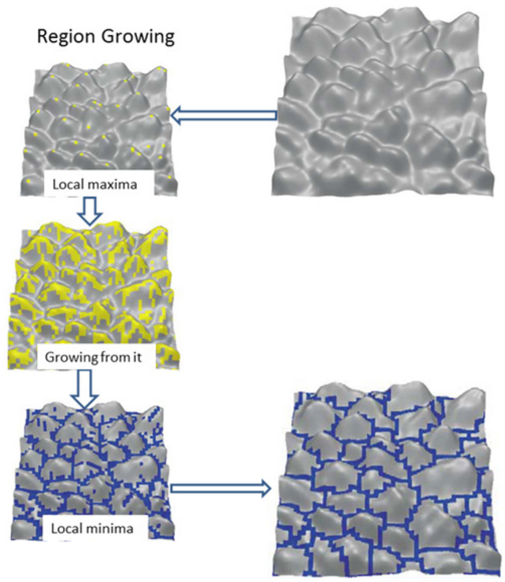

Figure 12. Basic concepts of two crown delineation approaches (adapted from Culvenor, 2002)

3.2.4. Validation of tree crown delineation

Validation of tree crown delineation used accuracy measures of checking the quality of segmentation which are commonly used for OBIA.

The quality of segmentation is related to quality of data (noise, spatial and spectral resolution) and the optimal customization of parameter settings, which enables the adaptation of segmentation results on target objects (Möller *et al.*, 2007). Validation of segmentation can be interpreted as 'an issue of matching objects' (Zhan *et al.*, 2005) where at least two hierarchical object-levels have to be considered in terms of their topological and geometrical relationships (Möller*, et al.*, 2007). Topological relationships of interests are 'containment' and 'overlap', whereas; geometric relationships can be determined by the comparison of object positions.

For segmentation validation, both relationships are considered. Especially:

- Relative area of intersection between segmented objects and reference objects (Möller*, et al.*, 2007)
- Distance between the centroids (Ke*, et al.*, 2010)
- 1:1 spatial correspondence (Gougeon & Leckie, 2006; Z Li *et al.*, 2009)
- Total number of pixel that segmented correctly (Coillie*, et al.*, 2008; Wang*, et al.*, 2004) are commonly used for validation of segmentation of tree crowns.

Clinton *et al.* (2010) summarized different segmentation accuracy measures by many researchers and modified relative area metrics by Möller *et al.* (2007). Over segmentation and under segmentation as defined by Clinton *et al.* (2010) are described as follows (Equation 1 and 2):

$$Over\ segmentation_{ij} = 1 - \frac{area(x_i \cap y_j)}{area(x_i)} \qquad \ldots 1$$

$$Under\ segmentation_{ij} = 1 - \frac{area(x_i \cap y_j)}{area(y_j)} \qquad \ldots .2$$

Where x_i is reference objects and y_j is corresponding segmented objects.

The value range of over segmentation and under segmentation is between 0 and 1, where over segmentation is equal to 0 and under segmentation is equal to 0 define a perfect segmentation, meaning the segments match the reference objects perfectly. Combination of over segmentation and under segmentation, D is interpreted as the 'closeness' measure to an ideal segmentation result, in relation to a predefined reference set (Clinton*, et al.*, 2010)(see Equation 3).

$$D = \sqrt{\frac{over\ segmenation^2 + under\ segmenation^2}{2}} \qquad \text{….3}$$

Value of D ranges from 0 and 1 and D equals to 0 implies a perfect segmentation.

For the purpose of detecting better tree crown delineation in this case, relative area measures modified by Clinton *et al.* (2010) and 1:1 spatial correspondence were selected for measure of accuracy. These accuracy measures were calculated for delineated tree crowns of each CFUGs. For 1:1 spatial correspondence accuracy measure, overall accuracy was calculated by comparing the number of 1:1 corresponding tree crowns of the reference and delineated tree crowns and total number of reference tree crowns.

Moreover, reference objects were manually delineated on the image as adapted in many tree crown delineation studies (Erikson & Olofsson, 2005; Gougeon & Leckie, 2006; Leckie*, et al.*, 2005; Wang*, et al.*, 2004). Manual delineation of tree crowns was done using Geo-Eye panchromatic image and MSS image with the same scale of 1:250 and crown width information for some trees.

To check the significant difference between the performance of Region Growing and Valley Following approaches, t-test was applied to the overall accuracies of tree crown delineation of these two approaches for each CFUGs.

3.2.5. Object based image classification

Classification consists in labelling the various components visible in an image (Martin *et al.*, 2006). According to the operators involved into the classification process, classification can be separated into unsupervised classification and supervised classification; according to classification element, it can be divided into pixel based and object based classification.

Pixel based classification assigns every individual pixel to a class based on reflectance variations across the spectral bands, or spectral signatures (Morales*, et al.*, 2008). Pixels with similar spectral reflectance are assigned to the same class. On the other hand, object based classification method uses not only spectral information, also, co-occurrence measures of texture (mean, variance, contrast, homogeneity and dissimilarity), spatial, contextual and semantic information can be used in the classification (Definiens 2009). Contextual and semantic information, for instance, spatial relationship between two objects, can be applied during the classification.

In object based classification, each class can be described by fuzzy rules, which base either on one-dimensional membership functions or on a nearest neighbour classifier. Both are supervised classification methods. While the first can be edited directly and enable the user to formulate knowledge about the image content, the latter needs appropriate sample objects to determine the desired class' properties. Samples can be selected manually (click and classify) or based on training area masks (Definiens, 2004).

Rule based classification

Each class of a classification scheme contains a class description, a set of fuzzy expressions allowing the evaluation of specific features and their logical operation. A fuzzy rule can have one condition or can contain a combination of some conditions, which have to be fulfilled for an object to be assigned to a class (Jacquin *et al.*, 2008). In eCognition the conditions are defined by expressions, which are inserted into the class descriptions. Expressions can be membership functions, similarities to classes or a nearest neighbour (Definiens, 2004).

Nearest neighbour classification

The nearest neighbour classification is applied to selected object features and is trained by samples. In comparison to pixel based training, the object based approach of the nearest neighbour requires fewer training samples. Samples are image objects which are the result of the segmentation process. After a representative set of sample objects has been declared for each class, the algorithm looks for the closest sample object in the feature space for each image object (Figure 13). If an image object's closest sample object belongs to Class A, the object will be assigned to Class A (Definiens, 2004).

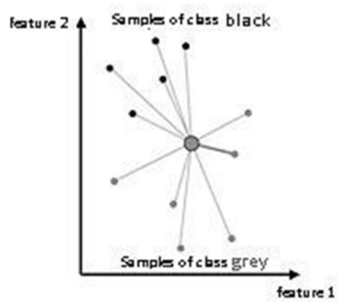

Figure 13. Nearest neighbour classification (Definiens, 2004)

Nearest neighbour classification was applied for species classification. Tree species, dominant in field collection data, were classified based on the segmented tree crowns having the highest accuracy and MSS image. Dominant species that are *Pinus roxburghii, Alnus nepalensis* and *Schima wallichiana* and other species were classified for the purpose of obtaining individual tree information. 70 % of the field sample data was used for training classification and the rest is used for validating the classification result. Classification was also done for forest type as broadleaf and needle leaf species.

To overcome the effect of shadow, shaded part was defined using aspect image from DEM and used for classification as one of the image layers. Based on the visualization of MSS image, north, north-west, west, and north-eastern aspects were classified as shadow affected area and the rest was classified as non-shadow area. Each class was classified both in the shadow affected area and non-shadow area and recoded into one class after classification.

Mean and maximum layer value of each MSS bands, panchromatic image, and aspect map for each object (delineated crown) were selected for feature space of nearest neighbour classification. Feature space of maximum layer value of an object was selected since it can represent the brighter sunlit pixel of a tree crown. This increases the separation of different classes, since mean layer value of a tree crown incorporates different proportions of the shaded side of a crown (Gougeon & Leckie, 2006; Leckie*, et al.*, 2005).

3.2.6. Field work

The purpose of fieldwork was to measure the AGB and identify trees that are recognizable in the image from the study area. This data was later used as the ground truth data for individual tree crown delineation, species classification, and validation of modelling the relationship of CPA and carbon stock of trees as well. Since some forest stand parameters such as volume and biomass are impossible to be measured directly in the field, relationships between directly measurable stand parameters (e.g. DBH, height) and biomass has to be established (Husch *et al.*, 2003). Thus, forest stand parameters, such as DBH and height were measured from the field and used for biomass estimation by applying allometric equations.

Pre-field work

Before collecting data from the field, reference data were prepared based on secondary data collection provided by ICIMOD project, Nepal. The stratified random sampling approach was applied to design the sampling for the fieldwork. Stratified random sampling helps to ensure that the sample is spread out over the whole study area (Thompson, 2002) and also aims at dividing a population into a number of parts which are homogeneous causing less sampling error and coefficient of variation (Cochran, 1977; Köhl *et al.*, 2006). Secondary data of local community forestry areas was used to facilitate the stratification. In total 116 sampling plot data were intended to be obtained from 58 stratums (CFUGs in Charnawati watershed area) by taking two samples in each (least number of sample unit in each strata (Cochran, 1977) in field work). Considering the difficulties of sample data collecting in a mountainous area, 50 sampling plots that have been collected by ICIMOD project in Nepal in July 2010 were added to the total ground truth data and the rest had to be collected during field work.

Moreover, a routine and navigation facilities (Ipaq and GPS), measuring tools for forest stand parameters were prepared for the field trip. For the identification of the recognizable trees on the map in the field, Geo-Eye enlarged maps of every plot with its surrounding areas were also printed before fieldwork.

Field data collection

Circular shape of plots having the smallest periphery in relation to the area and consequently, the lowest number of borderline trees was employed in the field. Plot size was 0.5 ha. Radius of the plots was depended on the slope of the plot. In the field, each tree having DBH larger than 10 cm was measured in each plot and information of other biophysical parameter such as the tree height and crown cover were collected. Moreover, 10 or more trees in each plot, that were recognizable in the Geo-Eye satellite image, were recorded. Recording sheet used in the field is shown in Appendix 2.
75 plots were intended to be collected during the fieldwork phase. However, due to time and budget limitations, and also the accessibility of the plots, 64 plot data were collected during the fieldwork.

Fieldwork data analysis

Species wise allometric equations were not available for the tree species in the study area, thus, for *Pinus roxburghii* allometric equations developed by Chaturvedi (1982) in Central Himalayan chir pine forest in Nainital, Uttarakhand, India (29° 24' N lat and 79° 28' E long) and for other species general allometric equation developed by Chave (2005) for tropical moist forest were used to calculate AGB (see equation 4 and 5).
Allometric equation for calculating biomass using DBH for *Pinus roxburghii* is shown below.

$$\text{Ln } W = a + b \text{ Ln } CBH \qquad \ldots 4$$

Where W: aboveground tree biomass [kg]

CBH: measured tree circumference at breast height [cm] (equals to DBH*π)
a and *b* (Table4) are parameters, specific to each different parts of tree (*Pinus roxburghii*).

Table 4**. Allometric relationship between the biomass of tree components and circumference to breast height [cm]** (Chaturvedi & Singh, 1982)

Biomass (kg per tree)	a	b	S y x	r^2	Correction factor
Bole	-6.418	2.598	0.064	0.985	0.0067
First order branch	-9.833	2.978	0.089	0.979	0.0129
Other branch	-9.338	2.63	0.105	0.963	0.018
Foliage	-6.111	1.872	0.086	0.952	0.012
All equations are significant at P > 0001. n = 26.					

Biomass allometric equation for other species is shown below.

$$AGTB = 0.0509 * pD^2 H \qquad \ldots 5$$

Where,
AGTB = aboveground tree biomass [kg]
p = wood specific gravity [kgm^{-3}]
D= tree diameter at breast height (DBH) [cm] and
H = tree height [m].
Wood specific gravity equals to 0.594 for mixed hardwood forests in Charnawati watershed, Dolakha, Nepal (ICIMOD *et al.*, 2010).
Furthermore, carbon stock of tree was calculated from AGB using 0.47 conversion coefficient (IPCC, 2006).

3.2.7. Regression analysis

The objective of regression analysis is to quantify the relationship between response variable and one or more explanatory variables. Quantitative relationship is expressed by an equation and its graphic representation (Husch*, et al.*, 2003). Coefficient of determination, the square value of the correlation coefficients (R^2) shows the percentage of variation in one variable that is associated with other variables which can be explained by the given equation.

Regression analysis is commonly used for biomass estimation studies (Lu, 2006). After calculating aboveground carbon stock using DBH information and allometric equations, relationship of aboveground carbon stock and CPA was analysed using regression analysis. Regression analysis was employed using the data of aboveground carbon stock as response variables and CPA as an explanatory variable.

Tree crowns that have 1:1 spatial correspondence with reference and delineated tree crowns having less error in terms of the relative area (less than 10 m^2) and correctly classified were used for modelling. The significance and the strength of this relationship was determined using evaluation dataset, which was 30 % of field dataset.

4. RESULTS

4.1. Descriptive analysis of field data

In total, forest stand parameter data of 4450 trees was collected from 114 plots in the Charikot watershed, Dolakha, Nepal. Out of these trees, 1240 trees were located on the image and digitized to the geo-information system. A total of 64 species were recorded (Appendix 3), 10 of which were the most common being 83% of the total trees in the field data (Figure 14).

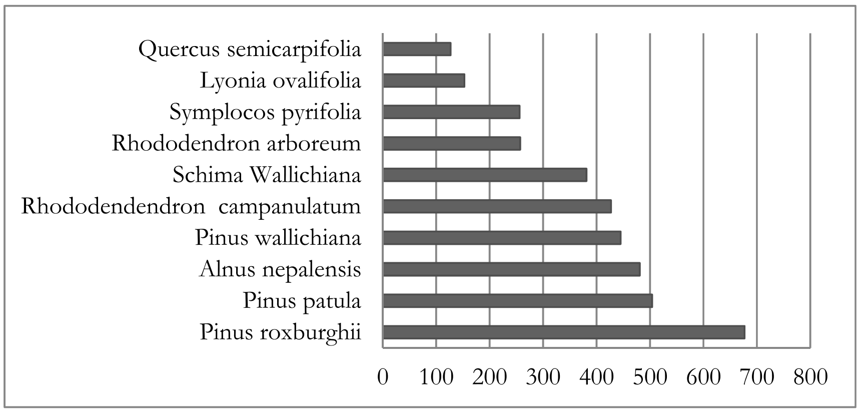

Figure 14. Frequency of the main species in the Charnawati watershed

Among these common species *Pinus roxburghii, Pinus patula* and *Alnus nepalensis* have the largest frequency (677, 504 and 481 respectively). DBH and height of the main species were analysed and presented by box-plot shown in Figure 15 for each species.

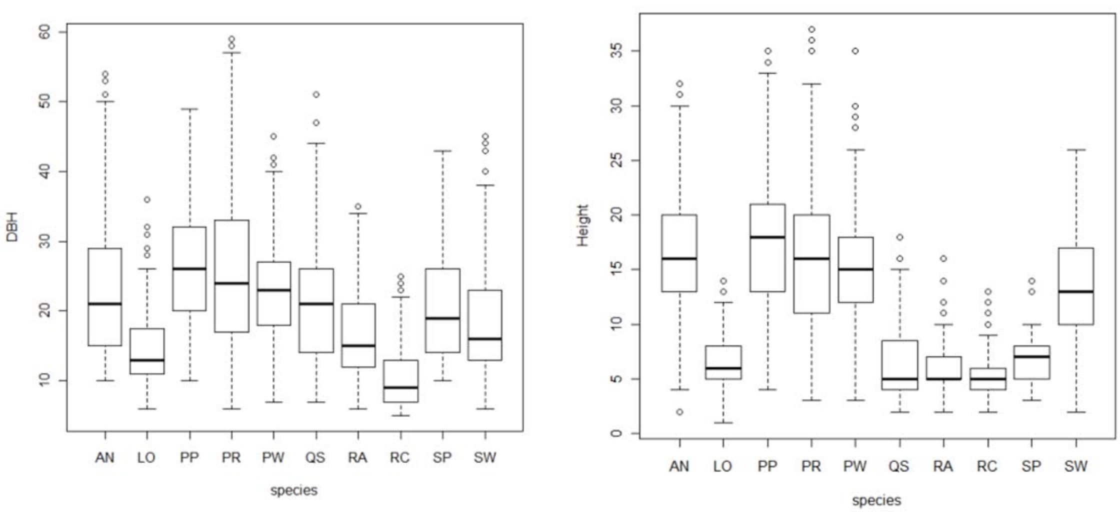

Figure 15. Box plots of DBH and height of the main species

(AN-*Alnus nepalensis*, LO-*Lyonia ovalifolia*, PP-*Pinus patula*, PR-*Pinus roxburghii*, PW- *Pinus wallichiana*, QS-*Quercus semicarpifolia*, RA- *Rhododendron arboretum*, RC- *Rhododendron campanulatum*, SP- *Symplocos pyrifolia*, SW- *Schima Wallichiana*)

On average, *Pinus patula* had the largest DBH and was the tallest followed by *Pinus roxburghii* and *Alnus nepalensis*. Moreover, these species have the highest variability in terms of DBH and height as well. On the other hand, *Rhododendron* family species such as *R.aboretum*, *R, camanulatum* and *Lyonia ovalifolia* had the least DBH and were the shortest in height. In particularly, heights of these species were not more than 6 m in average and also the variation of the height was less compared to DBH.

As mentioned in Chapter 3, the main analysis was done in central eastern part of Charnawati watershed due to the limitations of eCognition software. 21 plot data having measurement data of 601 trees and 209 trees identified on image were available from the field data in subset area of Charnawati watershed.
Subset area of Charnawati watershed covered 11 CFUGs and 9 species were recorded in this area. The most common species identified on image were *Pinus roxburghii, Alnus Nepalensis, Schima Wallichiana, and Engelhardicta spicata* (Figure 16).

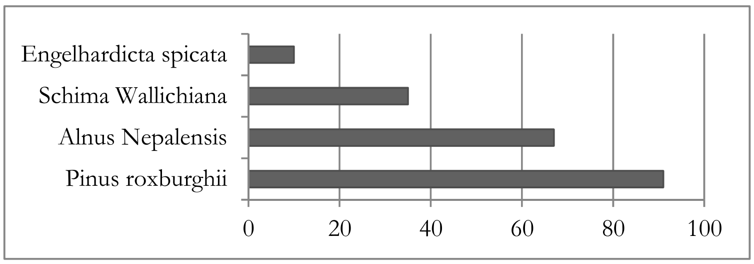

Figure 16. Frequency of main species identified on image in subset area of Charnawati watershed

The most frequent species in this area were *Pinus roxburghii* and *Alnus nepalensis* being 78% of total trees. Whereas, *Euriya cerasifolia, Gravelia robusta, Myrsine semiserrata, Berberis asiatica and Sapium insigne* had the least frequency having only 1-2 records. Figure17 presents the percentage of the main tree species identified in the image in each CFUGs.

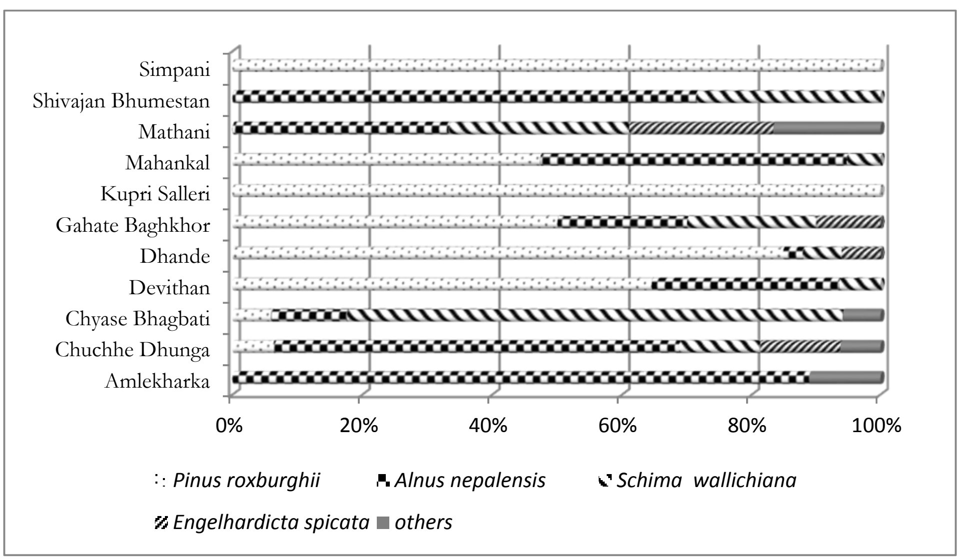

Figure 17. Percentage of the main tree species in each CFUGs

Pinus roxburghii was dominant in Simpani, Kupri Salleri, Dhande, and Devithan CFUGs, while, *Alnus nepalensis* was common in Shivajan Bhumestan, Chuchhe Dhunga, Amlekharka, and Mathani. According to the data collected in the field, almost all the CFUGs had mixed forest except in Simpani and Kupri Salleri.

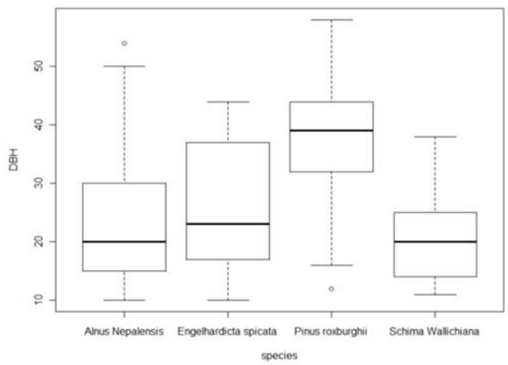

a. DBH of trees identified on the image

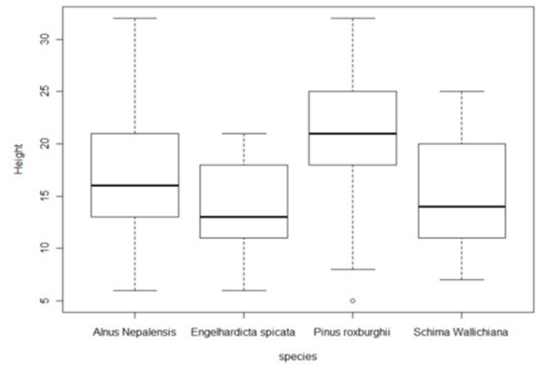

b. Height of trees identified on the image

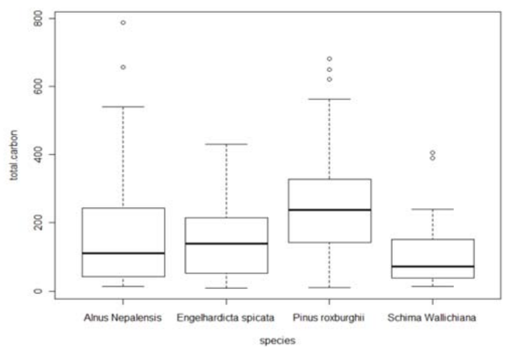

c. Carbon stock of trees identified on image

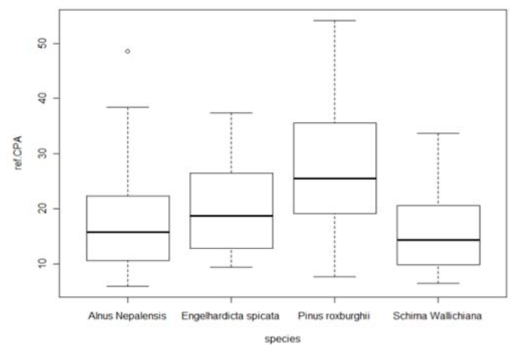

d. Digitized CPA of trees identified on image

Figure 18. Box-plots of measured parameter in subset study area

DBH, height, carbon stock and reference CPA of the main species were analysed and shown Figure 18. *Pinus roxburghii* had largest DBH, carbon stock and CPA (38 cm, 250kg/tree, and 25 m² respectively) and was the tallest (22 m) on average. Moreover, it had the biggest variability for all the parameters.

On the other hand, *Alnus nepalensis, Schima wallichiana*, and *Engelhardicta spicata* were more or less similar in terms of DBH (20-24 cm), carbon stock (80-120 kg/tree), and reference CPA (14-19m²) in average. Among these broadleaf species, *Alnus nepalensis* had the biggest variability for all the parameters.

4.2. Tree crown delineation

4.2.1. Tree crown delineation using Region Growing approach in eCognition

As a result of individual tree crown delineation using Region Growing approach, delineation of individual tree crowns of study area was done. Figure 19 shows the result of Region Growing approach on individual tree crown delineation in Mathani CFUG.

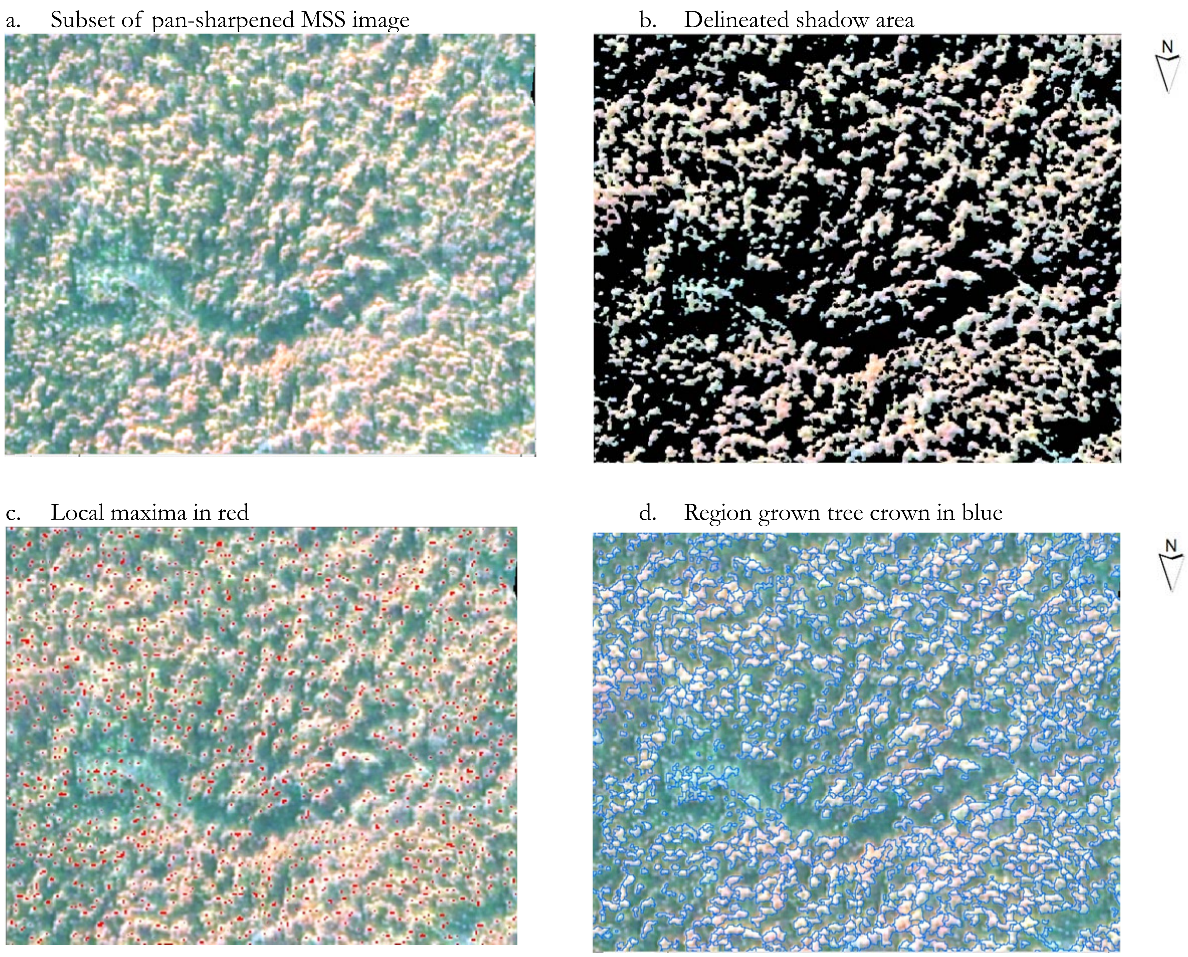

Figure 19. Tree crown delineation using Region Growing approach (scale 1: 3500).

Accuracy assessment of tree crown delineation of Region Growing approach was analysed using accuracy measures of D and 1:1 correspondence for 209 manually delineated reference tree crowns. Figure 20 shows accuracy measures of D of delineated crowns for each CFUGs. Overall for the whole study area, over segmentation was 0.28, under segmentation was 0.32, and D was 0.30. In other words, over segmentation error was 28 %, under segmentation error was 32 % and total delineation of tree crowns was 70 % accurate (30 % error). For the accuracy measure of 1:1 correspondence, 75 % of the total reference crowns were matching to the Region Growing crown delineation with 1:1 correspondence. In Amlekharka, D value was the lowest (0.20), where as in Shivajan Bhumestan, D value was the highest (0.38). Moreover, in Chyase Bhagabate and Amlekharka, where there was the dominance of broad leaf forest, D value was lower. On the other hand, D value was greater in Gahate Bhagabati, and Kupri Salleri, where there was the dominance of needle leaf forest.

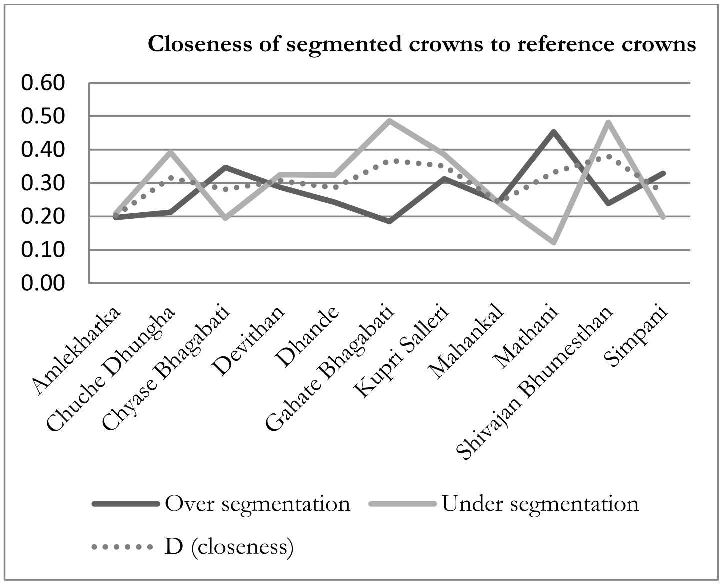

Figure 20. Accuracy measures of D of delineated crowns and reference crowns using Region Growing approach

1:1 correspondence of reference tree crowns and delineated tree crowns using Region Growing approach is shown in Table 5. In Amlekharkha, Chyase Bhagabati, Chuchhe Dhungha, and Mathani, more than 80% of trees have 1:1 correspondence to the delineated and reference crowns while, 1:1 correspondence was the least in Gahate Bhagabati and Kupri Salleri.

Table 5**. 1:1 correspondence of reference and delineated crowns from Region Growing approach**

	CFUG name	Reference	Delineated	1:1 correspondence	Percentage of 1:1 correspondence to reference crown
1	Amlekharka	9	9	9	100
2	Chuchhe Dhungha	16	17	13	81
3	Chyase Bhagabati	20	20	17	85
4	Devithan	21	26	16	76
5	Dhande	33	35	24	73
6	Gahate Bhagabati	20	20	13	65
7	Kupri Salleri	21	25	11	52
8	Mahankal	19	19	15	79
9	Mathani	18	17	16	89
10	Shivajan Bhumesthan	21	18	14	67
11	Simpani	11	14	8	73
	Overall	209	220	156	75

4.2.2. Tree crown delineation using Valley Following approach in ITC

The result of individual tree crown delineation using Valley-Following approach in some parts of Mathani CFUG is shown in Figure 21.

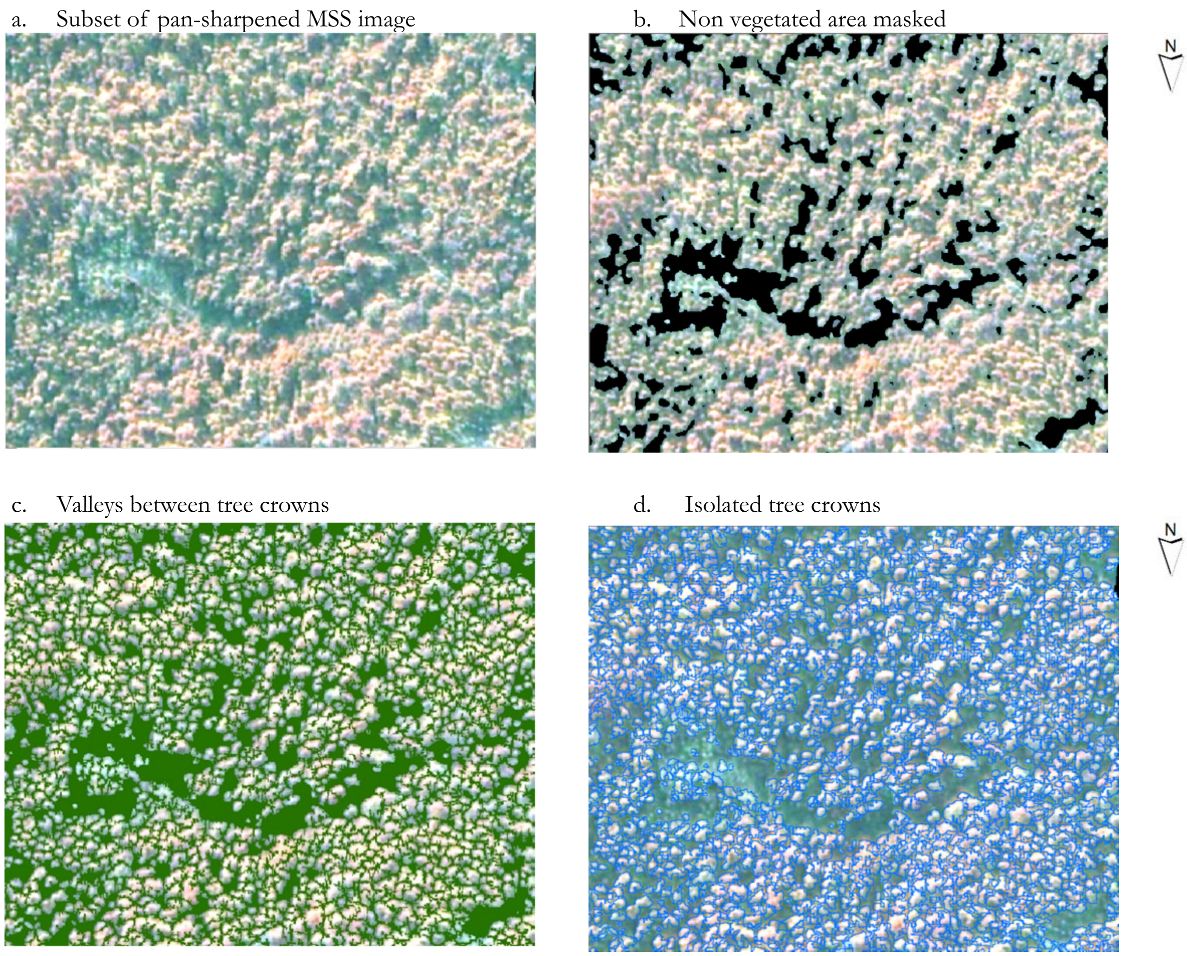

Figure 21. Tree crown delineation using Valley Following approach (scale 1: 3500)

Figure 22 shows accuracy measures of D of segmented crowns from Valley Following approach for each CFUGs. Overall for the whole study area, over segmentation was 0.41, under segmentation was 0.39, and D was 0.40. In other words, over segmentation error was 41%, under segmentation error was 39 % and overall accuracy was 60 % (40 % error). Table 6 shows the accuracy measure of 1:1 correspondence and 67 % of the total reference crown were matching spatially to the Valley Following crown delineation.

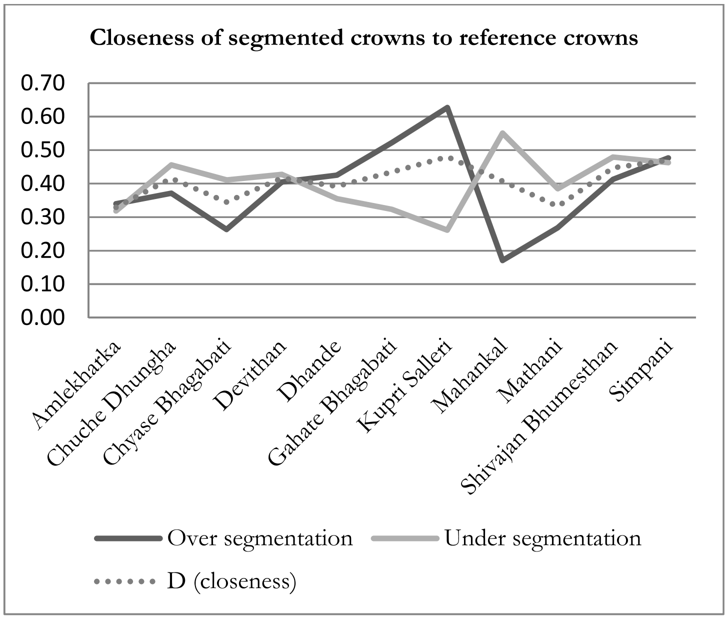

Figure 22. Accuracy measures of D of delineated crowns and reference crowns using Valley Following approach

In Amlekharka and Mathani, D value was the lowest (0.33), where as in Kupri Salleri, D value was the highest 0.48. Moreover, in Chyase Bhagabate, Mathani, and Amlekharka, where there was the dominance of broad leaf forest, D value was lower (0.33-0.35). On the other hand, D value was higher (up to 0.48) in Dhande, Gahate Bhagabati, Kupri Salleri, and Simpani, where there was the dominance of needle leaf forest.

Table 6. **1:1 correspondence of reference and delineated crowns from Valley Following approach**

	CFUG name	Reference	Delineated	1:1 correspondence	Percentage of 1:1 correspondence to reference crown
1	Amlekharka	9	10	6	67
2	Chuchhe Dhungha	16	20	13	81
3	Chyase Bhagabati	20	24	15	75
4	Devithan	21	29	15	71
5	Dhande	33	44	24	73
6	Gahate Bhagabati	20	30	12	60
7	Kupri Salleri	21	34	11	52
8	Mahankal	19	16	12	63
9	Mathani	18	21	14	78
10	Shivajan Bhumesthan	21	21	13	62
11	Simpani	11	15	6	55
	Overall	209	264	141	67

In Chyase Bhagabati, Chuchhe Dhungha, and Mathani, more than 75% of delineated tree crowns had 1:1 correspondence to the reference crowns. Whereas, 1:1 correspondence was the less than 60% in Kupri Salleri and Simpani.

4.2.3. Comparison of delineated crowns from Region Growing and Valley Following approaches

Figure 23 shows delineated crowns of Region Growing and Valley Following approaches (reference tree crowns in blue and delineated tree crowns in red).

a. Region Growing b. Valley Following

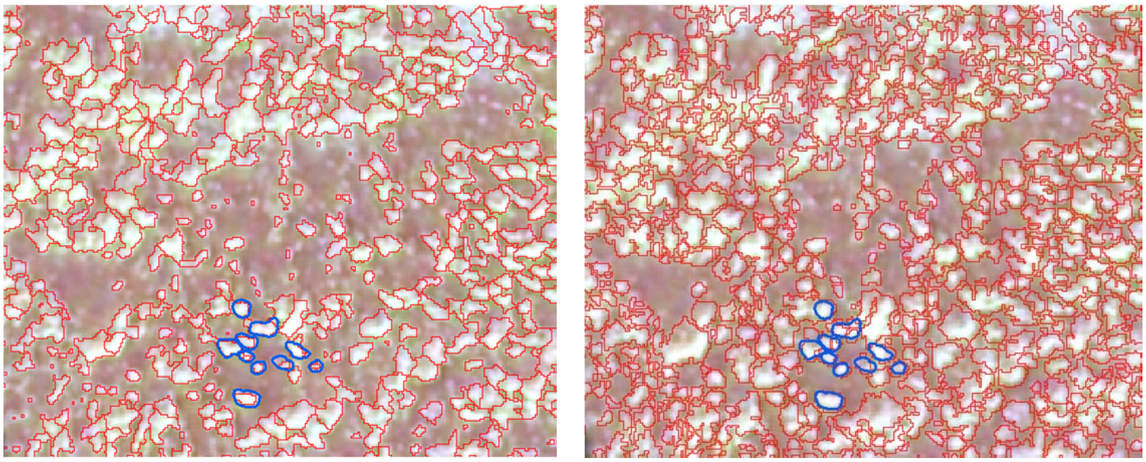

Figure 23. Delineated crowns of Region Growing and Valley Following approaches.

Figure 24 shows accuracy assessment of tree crown delineation of Region Growing and Valley Following approaches. Overall D value of Region Growing approach was 0.30 (max 0.37, min 0.2), while for the tree crown delineation of Valley Following approach, overall D was 0.40 (max 0.48, min 0.33). This result implies that tree crown delineation from Region Growing has less error and is more accurate than that of Valley Following approach. For 1:1 correspondence, also, delineated crowns from Region Growing were more accurate than Valley Following approach. Both the approaches resulted in lower accuracy of tree crown delineation in Kupri Salleri, where forest type was needle leaf.

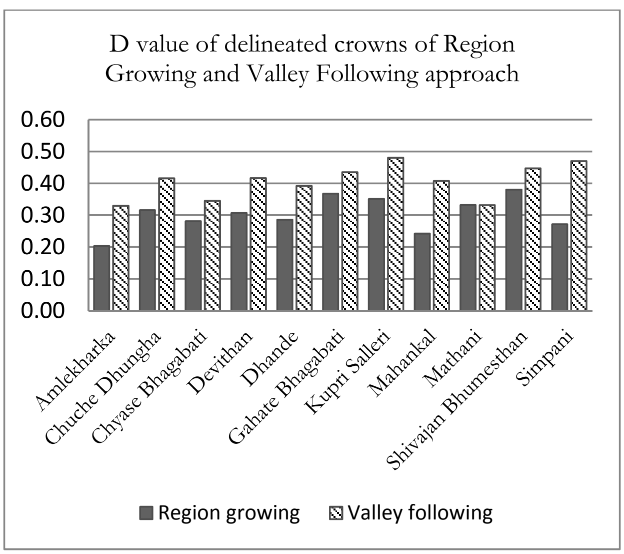

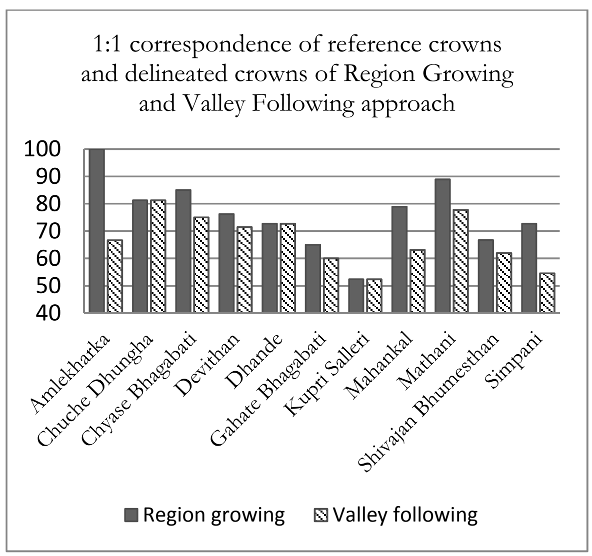

Figure 24. Accuracy assessment of tree crown delineation of Region Growing and Valley Following approaches.

To prove the hypothesis of research question two, t-test was used for the accuracy assessment of two tree crown delineation approaches. In both the accuracy measure (D and 1:1 correspondence), t-calculated value was higher than t-critical value with p value less than 0.05 when degree of freedom is 11.

This implies that there is a significant difference between the accuracies of tree crown delineation of Region Growing and Valley Following approaches. Thus, H1 hypothesis of a significant difference between the tree crown delineation of Region Growing and Valley Following approaches was accepted. In other words, tree crown delineation of Region Growing was significantly more accurate than that of Valley Following approach.

4.3. Object based image classification

Delienated tree crowns of Region Growing approach were classified into four main species types such as *Pinus roxburghii*, *Alnus nepalensis, Schima wallichiana,* and others (*Engelhardicta spicata* and others) with the help of MSS image, panchromatic image, and aspect image using nearest neighbour classification (Figure 25).

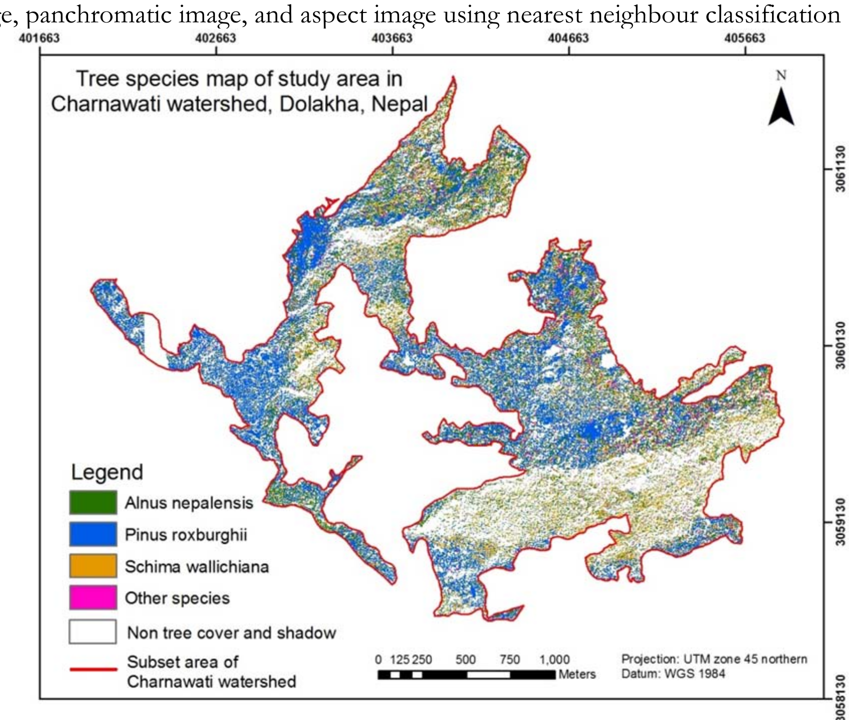

Figure 25. Tree species map of study area in Charnawati watershed, Dolakha, Nepal

From the classification result, the area and counts of each species class were calculated and presented in Table 7. In total 182 ha out of 343 ha was covered by trees and its crowns and others were non tree covers such as shadow and croplands *etc.* *Pinus roxburghii* was covering the largest area of total tree crown area followed by *Alnus nepalensis.*

Table 7**. Area of each species class and their counts**

Class name	Counts	Area (ha)
Alnus nepalensis	27547	55.71
Pinus roxburghii	29815	85.11
Schima wallichiana	13505	32.73
others	5387	8.50
Total	76254	182

The classification result was validated using 62 trees (20 *Alnus nepalensis*, 24 *Pinus roxburghii*, 11 *Schima wallichiana*, and 7 *Engelhardicta spicata* and others). Confusion matrix of errors and accuracies are shown in Tables 8 and 9.

Table 8. **Confusion matrix of errors of tree species classification**

Classification	Reference				
	Alnus nepalensis	*Pinus roxburghii*	*Schima wallichiana*	Others	**Total**
Alnus nepalensis	11	1	4	2	**18**
Pinus roxburghii	3	23	1	2	**29**
Schima wallichiana	6	0	5	2	**13**
Others	0	0	1	1	**2**
Total	**20**	**24**	**11**	**7**	**62**

Overall classification accuracy was 64.52% and kappa was 0.48. *Pinus roxburghii* was classified the most correctly with producer's accuracy of 95.8% and user's accuracy of 79.3%. Among for the broadleaf tree species, *Alnus nepalensis* was classified correctly with 55% producer's accuracy and 61.1% user's accuracy and other two classes were classified with poor classification accuracy. In general broadleaf tree species (*Alnus nepalensis, Schima wallichiana, Engelhardicta spicata etc.,*) were classified with poor accuracy and were overlapped more in feature spaces (Appendix 4). From the confusion matrix of errors, this was also clear that there was more classification error within those broadleaf species than *Pinus roxburghii.*

Table 9. **Accuracy assessment of tree species classification**

Class	Reference Total	Classification Total	Correct Total	Producer's Accuracy	User's Accuracy	Kappa
Alnus Nepalensis	20	18	11	55.00%	61.11%	0.42
Pinus roxburghii	24	29	23	95.83%	79.31%	0.66
Schima wallichiana	11	13	5	45.45%	38.46%	0.25
Others	7	2	1	14.29%	50.00%	0.44
Total	62	62	40			
Overall Classification Accuracy = 64.52%						**0.48**

Overall accuracy of species classification was not satisfactory as hypothesized and there was more confusion (error) between broadleaf tree species for classification.

Classification of forest type was also conducted by generalizing some species as broadleaf species (*Alnus nepalensis, Schima wallichiana*, and others species) and needle leaf species (*Pinus roxbhurghii*) and it was done using the same procedure as in species classification (Figure 26).

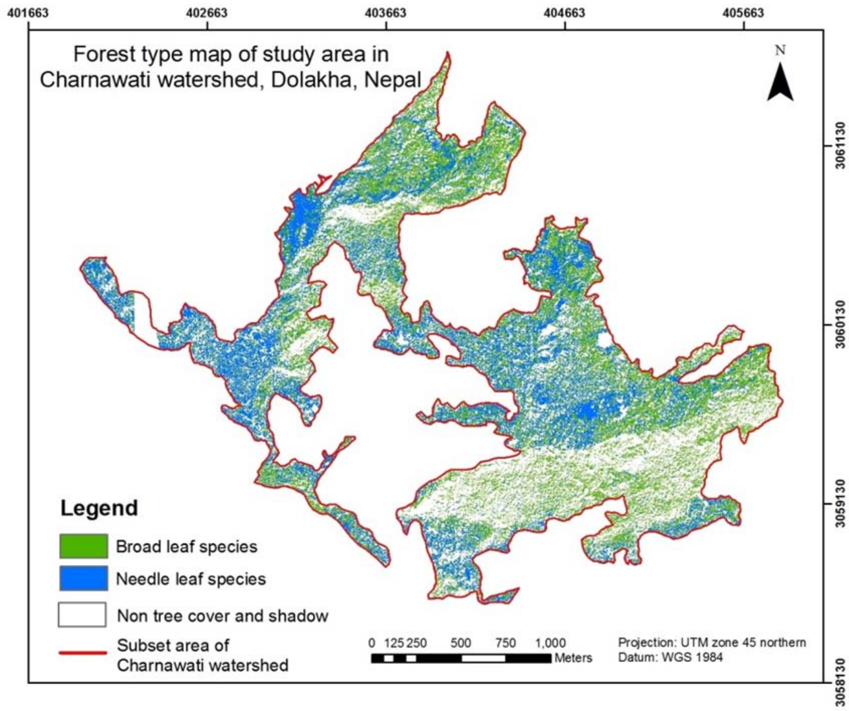

Figure 26. Forest type map of study area in Charnawati watershed, Dolakha, Nepal

Areas and counts of each forest type were calculated from the forest type classification (Table 10).

Table 10**. Area of each forest type class and their counts**

Class name	Count	Area (ha)
Broadleaf species	46629	97.45
Needle leaf species	29625	84.60
Total	76254	182

Classification result was validated using 62 trees (38 broadleaf and 24 needle leaf trees) and confusion matrix of errors is shown in Table 11.

Table 11**. Confusion matrix of errors of forest type classification**

Classification	Reference		
	Broadleaf species	Needle leaf species	**Total**
Broadleaf species	33	1	**34**
Needle leaf species	5	23	**28**
Total	**38**	**24**	**62**

Compared to tree species classification, the error of the classification was less for forest type classification. Overall classification accuracy also increased to 90.32% (kappa 0.80) and producer's and user's accuracy were more than 80 % for both classes (Table 12).

Table 12. **Accuracy assessment of forest type classification**

Class	Reference Total	Classification Total	Correct Total	Producer's Accuracy	User's Accuracy	Kappa
Broad leaf species	38	34	33	86.84%	97.06%	0.92
Needle leaf species	24	28	23	95.83%	82.14%	0.70
Total	62	62	56			
Overall Classification Accuracy = 90.32%						**0.80**

Species and forest type classification used separate classes in shaded and non-shaded areas. To determine the effectiveness of having these separate classes in classification, classification of species and forest type was also done without the separation of shaded and non-shaded. The results of these classifications are shown Tables 13 and 14 for comparison.

Table 13. **Error matrix and accuracy assessment of species classification when there is no separation of shaded and non-shaded classes**

		Reference Data				Total classified	Correct	Users' accuracy	Kappa
		Alnus Nepalensis	*Pinus roxburghii*	*Schima wallichiana*	Others				
Classified	Alnus Nepalensis	9	1	3	2	15	9	60.00%	0.45
	Pinus roxburghii	4	23	2	3	32	23	71.88%	0.54
	Schima wallichiana	7	0	5	1	13	5	38.46%	0.29
	Others	0	0	1	1	2	1	50.00%	0.44
Total Reference		20	24	11	7	62	38		
Correct		9	23	5	1	38			
Producers accuracy		45.00%	95.83%	45.45%	14.29%				
Overall Classification Accuracy = 61.29%									0.45

From Table 13 and 14, it is clear that use of separate shaded and non-shaded classes for each of the forest/species class was effective since the classification accuracy was decreased by 3-5% (Kappa 3-10%) when the separate shaded and non-shaded classes were not used for the classification.

Table 14. **Error matrix and accuracy assessment of forest type classification when there is no separation of shaded and non-shaded classes**

		Reference		Total classified	Correct	Users' accuracy	Kappa
		Broadleaf	Needle leaf				
Classified	Broadleaf	33	4	37	33	89.19%	0.72
	Needle leaf	5	20	25	20	80.00%	0.67
		38	24	62	53		
Correct		33	20	53			
Producer's accuracy		86.84%	83.33%				
Overall Classification Accuracy = 85.48%							0.69

4.4. Regression analysis

Descriptive statistics of the variables used for the carbon stock modelling are shown in Table 15.

Table 15**. Descriptive statistics of the variables used for modelling**

	Broadleaf			Needle leaf		
	Reference CPA	Segmented CPA	Tree carbon stock	Reference CPA	Segmented CPA	Tree carbon stock
Mean	16.89	16.76	227.18	26.67	26.27	305.48
Standard Deviation	8.15	10.34	165.65	10.19	7.66	151.49
Minimum	7.63	2.75	24.56	10.51	13.50	35.52
Maximum	48.59	46.50	791.45	45.66	44.75	605.86
Count	60			44		

Linear regression model was used to test whether segmented and reference CPA could explain the amount of carbon stock per tree for broadleaf species and needle leaf species since the classification result for single species was not satisfactory.

The result of a linear regression model explaining carbon stock of broadleaf and needle leaf (*Pinus roxburghii*) trees using reference CPA and segmented CPA from Region Growing approach is shown in Table 16.

Table 16**. Linear regression analysis for carbon stock of trees**

Broadleaf trees			***Needle leaf (Pinus roxburghii) trees***		
Regression Statistics	*Reference CPA*	*Segmented CPA*	*Regression Statistics*	*Reference CPA*	*Segmented CPA*
Multiple R	0.443312	0.349914	Multiple R	0.729781	0.577688
R Square	0.196525	0.12244	R Square	0.532581	0.333723
Adjusted R Square	0.176439	0.100501	Adjusted R Square	0.516463	0.310748
Standard Error	125.157	130.8	Standard Error	110.7804	132.2625
Observations	42	42	Observations	31	31
Coefficients			*Coefficients*		
Intercept	70.41992	121.004	Intercept	15.11297	-9.31496
slope	7.97212	5.002599	slope	11.10373	11.93296
P-value			P-value		
Intercept	0.129867	0.003394	Intercept	0.779059	0.912992
slope	0.003278	0.02311	slope	3.18E-06	0.000666

One way Analysis of Variance (ANOVA) test was employed to test the significance of the models and the result shown in Table 17 indicated that explanation of carbon stock by reference and segmented CPA was statistically significant at 95% confidence level.

Table 17. **ANOVA test of linear regression analysis for carbon stock of trees**

	Broadleaf trees					***Needle leaf trees***				
	Carbon stock explained by reference CPA					Carbon stock explained by reference CPA				
	df	*SS*	*MS*	*F*	*F Significance*	*df*	*SS*	*MS*	*F*	*F Significance*
Regression	1	153255.9	153255.9	9.78	0.003	1	1210.9	1210.9	61.2	1.25E-08
Residual	40	626571.4	15664.29			29	573.4	19.7		
Total	41	779827.4				30	1784.4			
	Carbon stock explained by segmented CPA					Carbon stock explained by segmented CPA				
	df	*SS*	*MS*	*F*	*F Significance*	*df*	*SS*	*MS*	*F*	*F Significance*
Regression	1	95481.95	95481.95	5.58	0.02	1	254099.3	254099.3	14.5	0.0006
Residual	40	684345.4	17108.64			29	507308	17493.38		
Total	41	779827.4				30	761407.3			

For all four models, explanation of carbon stock using reference/segmented CPA was significant. For broadleaf trees, the linear regression model resulted in R^2 of 0.196 for carbon stock and reference CPA relationship and R^2 of 0.122 for carbon stock and segmented CPA. On the other hand, for needle leaf trees (*Pinus roxburghii*), linear regression model resulted in higher R^2 (0.53) for carbon stock and reference CPA relationship than carbon stock and segmented CPA (0.33). Relationship between CPA and carbon stock of broadleaf and need leaf trees are shown as scatter-plots (Figure 27).

a. Broadleaf trees

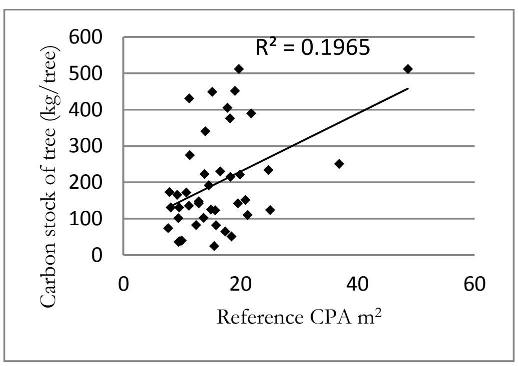

b. Needle leaf trees

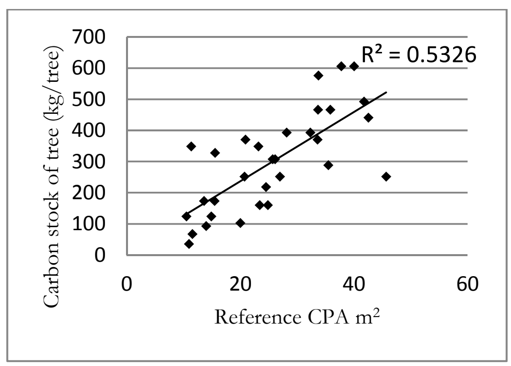

c. Broadleaf trees

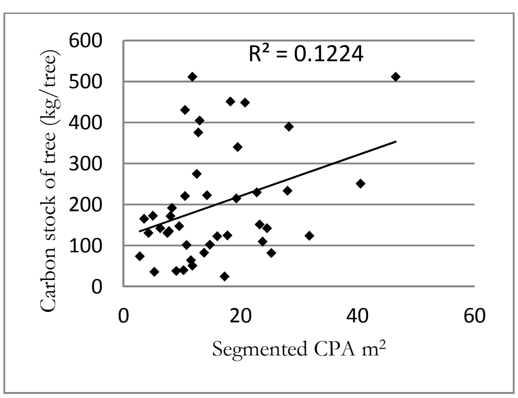

d. Needle leaf trees

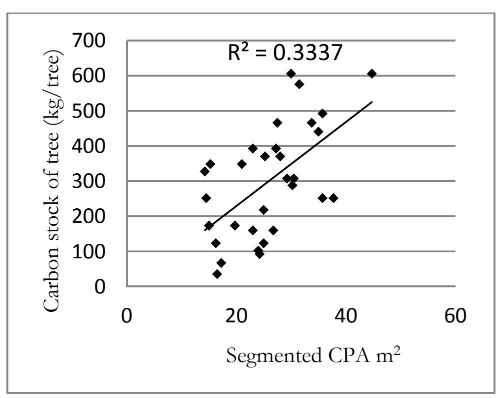

Figure 27. Scatter-plot graph showing the relationship between CPA and carbon stock of trees

Model validation

Linear regression models were applied to validate the relationship using evaluation data set. Observed and predicted carbon stock from linear regression models using reference and segmented CPA were plotted against each other and the co-efficient of determination was calculated as shown in Figure 28.

Similar R^2 values were found from model validation to model training. As mentioned above, R^2 of model validation of relationship between carbon stock of needle leaf trees and reference CPA was the highest (0.56), while, model validation of relationship between carbon stock of broadleaf trees and segmented CPA was the least (0.16).

In general, all models explaining the relationship of carbon stock of trees and CPA resulted in low R^2. Modelling carbon stock of needle leaf trees using reference and segmented CPA as an explanatory variable resulted in higher R^2 (0.56 and 0.34) and less RMSE (27.7% and 32.8%) respectively. On the other hand, modelling carbon stock of broadleaf trees using reference and segmented CPA resulted in less R^2 (0.26 and 0.16) and higher RMSE (65.2% and 68.5%) respectively.

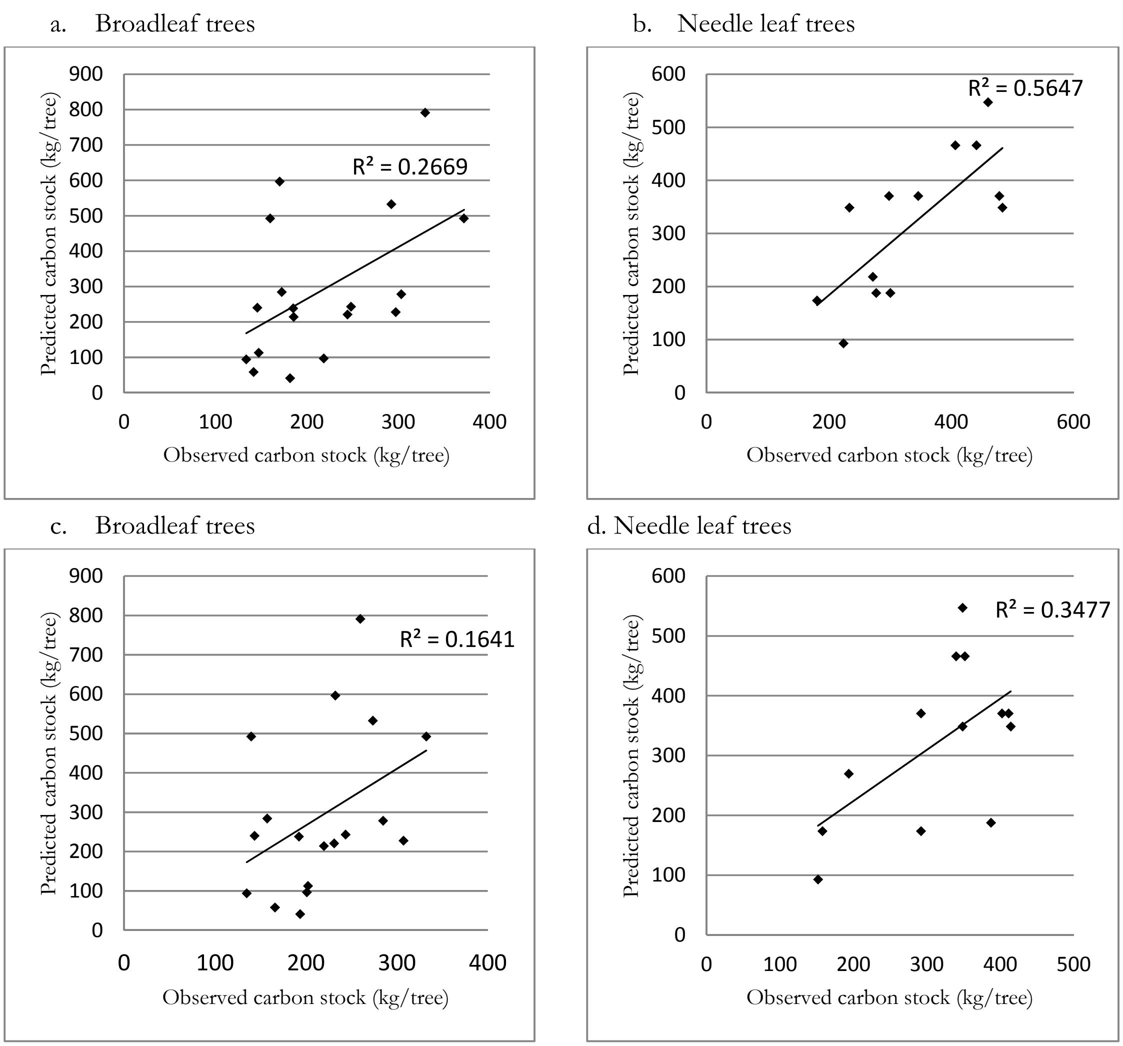

Figure 28. Scatter plot graph of predicted and observed values of validation trees.

5. DISCUSSION

5.1. Delineation of tree crowns

In this research, tree crown delineation was done using Region Growing and Valley Following approaches described in Section 3.1.3 and results are shown in Section 4.2.

Tree crown delineation using Region Growing approach resulted in accuracy of D of 0.30 (70 % accurate) with 75 % of 1:1 correspondence with reference tree crown in this study, whereas, tree crown delineation using ITC based Valley Following approach resulted in lower accuracy (D=0.40 or 60 % accuracy with 67% of 1:1 correspondence). The t-test proved that there is a significant difference between the accuracies of tree crown delineation of Region Growing and Valley Following approaches. This implies that tree crown delineation of Region Growing approach is significantly more accurate than that of Valley Following approach in this study. Examples of visually assessed well delineated tree crowns of both two approaches are shown in Figure 29 (reference crown in red, delineated crown in blue).

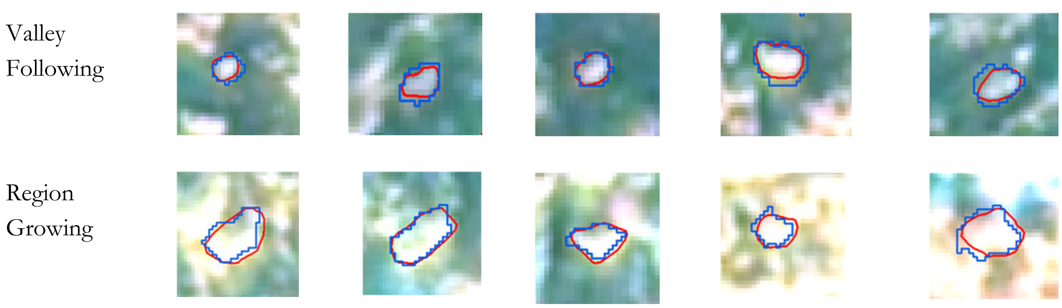

Figure 29. Examples of well delineated tree crowns.

ITC based Valley Following approach for tree crown delineation has been applied for different studies and effectiveness of this approach has been proven especially for plantation forests. For example, Gougeon (1995) first developed this approach and delineated tree crowns with 81% 1:1 correspondence with field data in coniferous plantation forest in Canada using MEIS-II image having 31 cm spatial resolution. Similar accuracy of delineation was also obtained by Gougeon & Leckie (2006) using IKONOS image of 83 cm spatial resolution with 7.4^{0} off-nadir view angle in softwood plantation forest. This approach also had been tested by Katoh *et al.* (2009) in Japanese plantation forests and resulted in 11.2% error. In this research, delineation of tree crown using Valley Following approach resulted in lower accuracy compared to previous studies. Unlike this study, previous studies were mostly done in plantation forest, while, when Valley Following approach was applied in old growth native coniferous forests, tree crown delineation accuracy was less (50-60%) (Leckie*, et al.*, 2005).

Region Growing approach using local maxima has also been intensively studied in different types of forests and has shown its usefulness. Tree crown delineation in naturally regenerated forest using aerial images captured almost at nadir achieved 70- 73% correct 1:1 correspondence by Brandtberg & Walter (1998) and Erikson (2003) respectively. Bunting & Lucas (2006) have achieved reasonable accuracy of crown delineation (72% correct when trees were well isolated) using CASI 14-band image in Australia. This study found similar accuracy of crown delineation (77% correct 1:1 correspondence) using Region Growing approach because naturally regenerated mixed forest was also studied in this research.

Moreover, techniques (developing rule-set in eCognition) used for Region Growing approach was similar to the study of Bunting&Lucas (2006).

Both the Valley Following and Region Growing approach for tree crown delineation have succeeded in different conditions, but comparison of the performance of these approaches has rarely been done. Ke & Quackenbush (2008) have compared the ability of three tree crown delineation approaches in deciduous and coniferous plantation sites using natural colour aerial image having 60 cm resolution and reported that Region Growing approach gives the best delineation with an accuracy of up to 78% 1:1 correspondence, whereas, Valley Following approach gives an accuracy of up to 66% 1:1 correspondence. This study also proved that Region Growing approach is better than Valley Following approach for tree crown delineation in mixed forest. This is because Valley Following approach is more favourable to coniferous plantation trees having conical crowns (Gougeon, 1995) and Region Growing approach has proven to be effective for the more complex forest structure of naturally regenerating forests as mentioned above.

Limitations of Valley Following approach such as an existence of shadow in between the trees and high view angle of image capture (Gougeon, 2010) could be the reason for results of lower accuracy when compared with Region Growing approach since shadows between trees are less common in naturally regenerated mixed forests and broadleaf forest stands. Gougeon & Leckie (2006) have also noted that Valley Following approach gives less success rate for broadleaf forests compared to coniferous, as their complex crown shapes make the presence of sufficient shade between them less common. Moreover, Leckie *et al.* (2005) discussed the difficulty of good tree crown delineation on sites with variable tree sizes with Valley Following approach since it was observed that when good delineation was achieved on smaller crowns, very large crowns tend to be severely broken up into several crowns. In this study, splitting of bigger crowns was also observed. Due to the less shadows in broadleaf forests, clusters of tree crowns were delineated instead of individual tree crowns in some areas when Valley Following approach was used (Figure 23 b).

On the other hand, Region Growing is more flexible in detecting tree crowns with varying sizes (as in this case) since this approach uses both features of local maxima as seeds for growing and local minima as restriction of the crown growing expansion (Ke & Quackenbush, 2008). However, Region Growing approach is most suited to crown delineation in pre-mature forest canopies where trees have a well-defined crown shape, but it will give less accuracy for complex forest types (Culvenor, 2002). Bunting & Lucas (2006) also stated that crowns of some trees could not be separated simply due to close proximity of their crowns or high density in the understory.

Most of the studies on tree crown delineation (Gougeon & Leckie, 2006; Katoh*, et al.*, 2009) have been done in plantation forest where thinning process is practiced regularly thus, having regular distances between the trees unlike the study area in this research. Moreover, most delineation algorithms have been developed for a specific forest type and species composition of stands, and therefore, are less likely to be applicable to natural forests (Bunting & Lucas, 2006). The performance of these algorithms may reduce, especially in sites having photo-synthetically active understory and ground surface vegetation, multi-layered forests of high density and presence of intermingled crowns (Bunting & Lucas, 2006; Erikson, 2003; Gougeon & Leckie, 2006). In this research, high density understory and multi-layered forests were also observed in the field and this could explain lower accuracy of tree crown delineation in some CFUGs. This trend agrees with other studies. For example, Bunting & Lucas (2006) observed that accuracy of crown delineation was greater than 72% when trees were well isolated, while it decreases (48-71%) when trees occurred in multiple strata having dense understory. Palace *et al.* (2008), moreover, has done tree crown delineation in Amazon tropical forests, but accuracy of delineation couldn't be checked due to difficulties in geo-locating trees under the dense multiple layers. This suggests that delineations are less successful as the structural complexity of forest increases. Thus, considering the complexity of natural mixed forest, accuracy of tree crown delineation obtained this study was satisfactory.

In this study, over segmentation was 0.28 and 0.41 for delineation of Region Growing and Valley Following approaches respectively; while under segmentation was 0.32 and 0.39 for the delineation of two approaches respectively. Over segmentation represents smaller or missing crown delineation than the reference - similar to omission error, and under segmentation represents bigger or new crown delineation - similar to commission error. Both over segmentation and under segmentation of crown delineation of Region Growing was less than that of Valley Following approach, thus meaning less error compared to Valley Following. Table 18 shows examples of errors of commission and omission for the crown delineation of Region Growing and Valley Following approaches based on visual assessment (reference crowns in red and delineated crowns in blue).

Table 18**. Examples of crown delineation errors**

Error of omission		Valley Following	Region Growing
a	small isolated crowns with a signal too weak to be detected		
b	two proximal crowns delineated as one		
c	crowns with weak signal are further reduced by delineation		
Error of commission			
d	big branch clusters in crown detected and delineated as two crowns	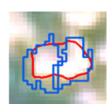	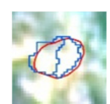
e	crowns delineated as bigger than they are due to low lying vegetation or understory or close proximity to smaller crowns		

The largest source of omission error of delineation was small trees not being delineated due to weak signals and selected smoothing factor in the shadow affected areas (Figure 23). This trend was also observed by Pouliot (2005). Moreover, close proximities of multiple crowns causing a joint crown after delineation was also common, especially for Valley Following approach due to insufficient shadows between trees. This error of omission has been commonly observed by other researchers (Bunting & Lucas, 2006; Pouliot*, et al.*, 2005). In addition, errors of commission have been identified by researchers as larger crown often split up due to their irregular crown shapes (Katoh*, et al.*, 2009) and the larger crowns may enclose a smaller one, causing bigger single crowns (Erikson, 2003). This could explain errors of over segmentation and under segmentation found in this study. However, crown delineation errors related to crowns overtopped by taller trees and intermingled crowns remains uncertain, since those are obscured from the view of satellite image (Bunting & Lucas, 2006; Katoh*, et al.*, 2009; Palace*, et al.*, 2008)

In contrast to the findings of Gougeon (1995) that Valley Following approach is more favourable in condition of needle leaf forest than hardwood crowns, D value (error) in this research was higher (Figure 18 and 20) in some CFUGs where there was a dominance of broad leaf trees (Figure 15) for both the approaches. The reason could be that these crown delineation approaches result in more error in bigger crowns such as splitting up or enclosing a smaller crown as discussed above. As pine trees are much bigger than other broadleaf trees in terms of DBH, carbon stock and CPA in this study area (Figure 16).

Delineation of tree crowns in this study was comparable with other researchers in respect of 1:1 correspondence of delineated and reference tree crowns. Even though most of the studies on tree crown delineation have used 1:1 correspondence as an accuracy measure for the performance of crown delineation approach, in this study accuracy measure of D focusing on relative area of the delineated tree crown and reference tree crown was also used since delineated CPA was intended to be used for modelling carbon stock of a tree. Similarly, Ke *et al.* (2010) used relative area of intersection of reference and segmentation as an accuracy measure for delineation of forest stand.

5.2. Object based image classification

Delineated tree crowns were further used for species and forest type classification described in Section 3.1.5 and results are shown in Section 4.3.

Species classification using Geo-Eye MSS image and delineated tree crowns resulted in overall accuracy of 64.5% and Kappa 0.48 for four species classes of *Alnus Nepalensis, Pinus roxburghii, Schima wallichiana,* and *Engelhardicta spicata* and others. Classification accuracy increased (overall accuracy 90.3% and Kappa 0.80) when species were generalized into broadleaf and needle leaf species.

Tree species classifications using high resolution imagery have been conducted by many researchers and satisfactory results have been found. For instance, Katoh (2009) and Gougeon & Leckie (2006) classified five needle leaf classes and one broadleaf class on the individual tree level with 78 % and 59% accuracy respectively using four band VHR image. Classification accuracy increased considerably (92.8% for six species) when CASI hyper-spectral image was used on the forest stand level (Leckie*, et al.*, 2003). Moreover, this research obtained higher classification accuracy for forest type with only two classes. This trend is commonly observed by other researchers. For example, Erikson (2004) has done species and forest type classification in naturally regenerated forests using aerial image of 3 cm resolution and obtained 77% accuracy for four species and 91% accurate classification for broadleaf and needle leaf two classes. Similarly, Brandtberg (2002) got 67% classification accuracy with a priori information and 87% for broadleaf and needle leaf classes using 10 cm resolution aerial image of naturally regenerated forests. These accuracy values reported in the literature cannot be compared to the results in this research. The reason is that the datasets are acquired from various forest types with different degrees of spectral overlap between the species, and with varying amount of automatic or manual delineation errors in the input data. Nevertheless, the range of previously reported accuracy value suggests that the species and forest type classification in this study is comparatively successful.

The main issue of species classification reported by literatures was spectral overlap between different species which creates confusion in classification (Brandtberg & Walter, 1998; Leckie*, et al.*, 2003). In this research, this trend was also observed specially, broadleaf species of *Alnus nepalensis* and *Schima wallichiana* and other species were spectrally overlapped. While, there was less overlap between *Pinus roxburghii* and other broadleaf species (Appendix 4a). Leckie *et al.* (2004) and Gougeon & Leckie (2006) observed considerable spectral overlap between the signatures of the different species, especially white pines and spruce, whereas less spectral overlapping was recorded between broadleaf and needle leaf species (Brandtberg, 2002). On the other hand, when CASI hyper-spectral image was used there was less spectral overlap thus, resulting in high classification accuracy since it provides better spectral resolution (Leckie*, et al.*, 2003).

Considering spectral variability of tree crown level in high resolution images, the usage of signature of lit side of the tree crown is proven to be an effective classification method (Gougeon, 1995). Lit side is the brighter side of the tree crown. Compared to using a mean spectral signature of a full crown, using lit side reduces spectral variability of a crown influenced by different proportions of shaded side, thus gives more separation of spectra (Leckie*, et al.*, 2004). In this research, brightest pixel of the tree crown was also used for classification. Compared to the mean spectral value of the tree crown, this can help for the spectral separation of the species, in particular, in NIR band (Appendix 4 a and b). Studies have also reported that using lit side signature helps to improve classification (Gougeon, 1995; Gougeon & Leckie, 2006; Leckie*, et al.*, 2003).

Effect of shadow on remotely sensed image at both the tree level and landscape level has been identified as an issue affecting species classification results. Effect of shadow on the tree level and how to overcome this issue has been discussed above. Leckie *et al.* (2005) discussed that the effect of shadow on remotely sensed image in landscape level due to topography and low sun elevation during acquisition time influences the spectral information of species and thus, affects classification. To accommodate this issue, classification of separate shaded classes was suggested and its efficiency was proven by Leckie *et al.* (2005). In this research, thus, separate classes of the shaded area were added to the each species class and it helped to improve the classification. Classification accuracy was improved by 3-5% (Kappa 3 to 10%) (Table 13 and 14) when shaded classes were added. Shaded area was determined by aspect data from DEM. Usage of topographic data such as elevation, slope and aspect is also recognized to be an effective way of improving classification. For instance, Ke *et al.* (2010) noted that classification accuracy increases by up to 20% when LiDAR derived topographic information including slope and aspect used for classification.

Quality of tree crown delineation also affects species classification results. Especially, when there are omission and commission errors of tree crowns, mean pixel value or lit pixel values of tree crowns are influenced. Erikson (2004) and Brandtberg (2002) discussed that delineation error of tree crowns can affect the classification system and with better segmentation, the classification can most probably be better. Leckie (2005) investigated the influence of quality of tree crown delineation and noted that classification accuracy was higher (40-70%) for well delineated tree crowns, while classification accuracy was much lower for all crowns when poorly delineated ones are included. Furthermore, the poor resolution of MSS images e.g. IKONOS (4m) can affect species classification on the individual tree level (Gougeon, 1995; Pouliot *et al.*, 2002).

5.3. Modelling the CPA and carbon stock relationship

Delineated CPA was further used for modelling the relationship of CPA and carbon stock of tree species as an explanatory variable (described in Section 3.1.7.) and the outcome of the models is shown in Section 4.4.

Modelling the relationship of carbon stock of trees and CPA was done and validated for broadleaf and needle leaf species (*Pinus roxburghii*). The model validation result shows that there is a poor relationship between carbon stock of trees and delineated CPA for both broadleaf and needle leaf species (R^2 is 0.16 and 0.35 respectively). When the reference CPA was used for modelling, R^2 was relatively higher (0.27 and 0.56 respectively), but strong relationship of CPA and carbon stock of trees has not found. Simple linear regression was applied for modelling the relationship of CPA and carbon stock of trees since mostly sparse forest cover was observed by ICIMOD (2010) in Charnawati watershed. The reason is that DBH and CPA has linear relation in sparse forest since competition from neighbouring trees is less (Foli *et al.*, 2003; Shimano, 1997).

Studies about the relationship between CPA and carbon stock or biomass of tree species, studied in this research, have been rarely done. Sharma (1999) studied the relationship between crown diameter and DBH of *Alnus Nepalensis* which were subjectively selected in the field measurement and stated non-linear model can explain this relationship with 78% of a coefficient of determination, yet the mechanistic meaning of the non-linear model was not explicitly explained. Hemery *et al.* (2005) studied the crown diameter and stem diameter relationship for different species of broadleaved trees in UK and obtained more than 0.8 R^2 of linear relationship in plantation forest. Moreover, allometric equation of DBH and crown diameter was developed for Amazon forest with R^2 of 0.57 (Palace*, et al.*, 2008). For needle leaf trees, Kuuluvainen (1991) modelled the relationship between CPA and AGB of Norway spruce plantation and obtained R^2 of 0.79. Furthermore, Avsar (2004) obtained R^2 of 0.74 from a non-linear relationship between crown diameter and DBH for *Pinus brutia*. In this study, the relationship of the reference CPA digitized from VHR image and carbon stock of both needle leaf and broadleaf trees resulted in weaker relationship than compared to previous studies.

Modelling biomass and carbon stock using CPA or crown diameter from VHR image gives relatively less accuracy compared to the field measured CPA or crown diameter. Robustness of modelling biomass and carbon stock density using Quickbird and LiDAR imageries have been proven by Gonzalez (2010). However, many studies resulted in lower accuracy of modelling the relationship of crown width or CPA and DBH or biomass. For example, Song *et al.* (2010) used crown diameter from Quickbird and IKONOS image with up to 18^0 of off-nadir view angle to predict DBH estimates and obtained R^2 of 0.5-0.6 for all species. Moreover, Zhang *et al.* (2010) and Wulder *et al.* (2000) achieved R^2 of 0.3-0.35 from the linear relationship of DBH and automatically delineated crown diameter in naturally regenerated forests, while Brandtberg and Walter (1998) did not find a significant relationship from field and image measured crown diameters. The strength of the relationship of carbon stock of tree and automatically delineated CPA found in this research was also comparatively lower than previous studies. The following paragraph will show more explanations.

R^2 of models using delineated CPA were lower than that of models when the reference CPA used and this can be explained by the error of the tree crown delineation. Song *et al.* (2010) suggested that error from the delineation of tree crowns can affect the result of modelling DBH and CPA relationship. However, a good relationship of carbon stock of trees and CPA were not found even when the reference CPA used in this research. Because, both of reference CPA and delineated CPA variables were derived from satellite images since reference CPA was digitized from Geo-Eye image. There can be a good relationship between CPA and carbon stock of a tree in study area, but it was not found from this study using VHR Geo-Eye imagery. The reason could be that the effect of topography, sun elevation angle and off-nadir viewing angle of image change the real tree crown size on remotely sensed image. Song *et al.* (2010) stated that although trees are always vertical regardless of whether they grow on a slope or on a flat surface, topography and off-nadir viewing angles can make the apparent tree size in the image different from the real tree size. Detailed explanation of these effects can be found in following section.

Model R^2 of the relationship between carbon stock of tree and CPA of needle leaf species was higher compared to that of broadleaf species. Similarly, Song *et al.* (2010) also observed stronger relationship for needle leaf species from the modelling of crown diameter from the field measurement and VHR image. However, in this case effect of shadow influenced on the relationship of carbon stock of broadleaf tree and CPA. The reason is that *Pinus roxburghii* mostly grows in southern and eastern aspects which are not affected by shadow on the image (Applegate *et al.*, 1988), whereas 60 % of broadleaf trees used for modelling were located in shaded area (Appendix 5). It was clear that these trees in the shaded areas were affecting the result of modelling carbon stock of broadleaf tree and CPA relationship since the correlation of CPA and carbon stock was much higher for broadleaf trees that are located in non-shaded areas (Appendix 5).

5.4. Source of errors related to analysis

Factors such as sensor view angle, sun elevation and topography have a significant effect on the radiometric and geometric properties of the tree crowns on VHR image. This can affect the allometric relationship of tree crown and other forest stand parameters such as biomass and DBH (Pouliot, *et al.*, 2005). Culvenor (2002) suggested that real geometric and radiometric properties of tree crowns can be detected best with small off- nadir view angles (less than 15 degree) and higher solar zenith angles. Source of errors related to the detection of real geometric and radiometric properties of tree crowns are discussed in the following sub sections.

5.4.1. Effect of shadow

Shadow at tree crown level (sun angle and height)

Effect of shadow influences the geometry of tree crowns and the magnitude of this effect depends on the sun azimuth and elevation angle at the time of the imagery (Leckie, *et al.*, 2005). Presumably, tree crowns would have a regular circle shape at the nadir view and solar zenith angle but such ideal situation can be rarely found (Pollock & Woodham, 1996). Based on the way that how the tree crown looks on satellite images with different sun elevation angle and view angle, researchers have developed the template matching algorithm for detecting tree crowns (Olofsson, 2002; Pollock & Woodham, 1996). In this study, Geo-Eye imagery having sun angle azimuth 163.5^0 and elevation 45^0 captured at 10:57 local time was used. Low sun elevation angle resulted in a shaded side for the tree crowns which makes it difficult to be distinguished on remotely sensed image. This was also observed by Erikson (2004). Culvenor (2002) showed that better tree crown delineation can be done with higher sun elevation. Figure 30a shows templates of different tree crowns from the nadir view angle when the sun angle is not at the zenith (Erikson & Olofsson, 2005) and Figure 30b shows examples of irregular shaped tree crowns similar to Figure 30a in which both low sun elevation angles and off-nadir view angle have influenced.

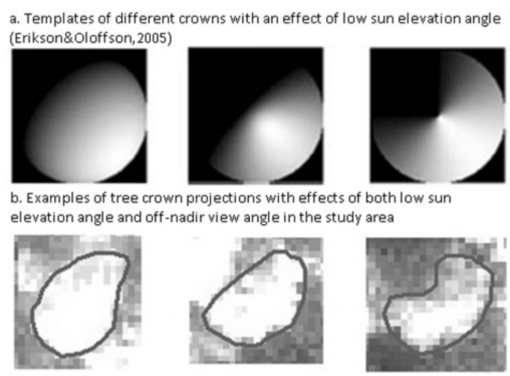

Figure 30. Examples of irregular shaped tree crowns and templates.

Shadow at landscape level

Shadow at the landscape level affects both the radiometric and geometric properties of the tree crown and this can happen due to steep topographic slope and aspect. At the landscape level, differences in illumination due to topography cause shaded and sunlit slopes that make it hard to effectively extract an accurate CPA (Culvenor, 2002). In shaded part, it affects not only the brightness value of tree crowns, also it influences to the size and shape of the crown since low brightness values cannot be separated accurately from the background (Culvenor, 2002; Leckie, *et al.*, 2005). Due to steep topography, effect of shadow was considerable and mostly occurred in western, north-western, northern, north-eastern aspects since the sun angle was 163^0 (south-south-eastern SSE). Besides, in shaded sides it seems that there was more space between the trees than in non-shaded sides in Geo-Eye image (Figure 31). However, dense forest was observed by ICIMOD (2010) especially in this part. This means that due to shadow effect small tree crowns cannot be observed or tree crowns look smaller thus creating more space in the image. This can explain why there was a very poor relationship between carbon stock of trees and CPA in shaded areas for broadleaf species.

Culvenor (2002) also discussed that the effect of shadow can be even more complex and unsystematic in mixed stands due to the size or trees, mix in heights and uneven stem and gap distribution. Tiede *et al.* (2008) also observed hindering of tree crowns in steep and shaded condition.

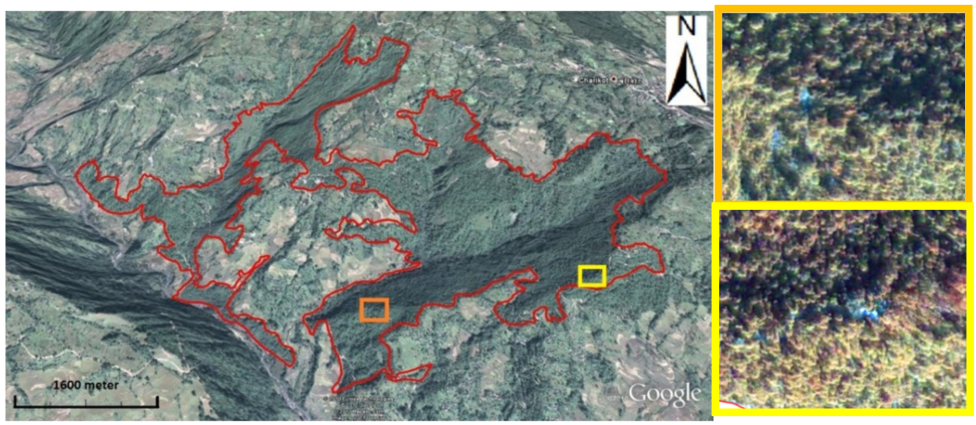

a.Quick-bird image of Google-Earth of the study area in 3D

b. Corresponding subset images of Geo-Eye

Figure 31. Screenshot showing shadow effect at landscape level and apparent increased tree spacing from the ridge due to the shadow effect

5.4.2. Effect of inclination angle of image acquisition

View angle during image collection also influences the shape of tree crowns on the image and the quality better delineation (Leckie*, et al.*, 2005). View angle nearer to the nadir result in circular crown shape on the image when the solar elevation angle is high, whereas, tree crown display crescent shape in off-nadir images (Leboeuf*, et al.*, 2007). In this study, Geo-Eye image having 25.4^0 off-nadir view angles was used and together with steep slopes (up to 56^0 degrees) it complicated the projection of tree crowns on the image even more. This resulted in irregular shapes of tree crowns in VHR image (Figure 32).

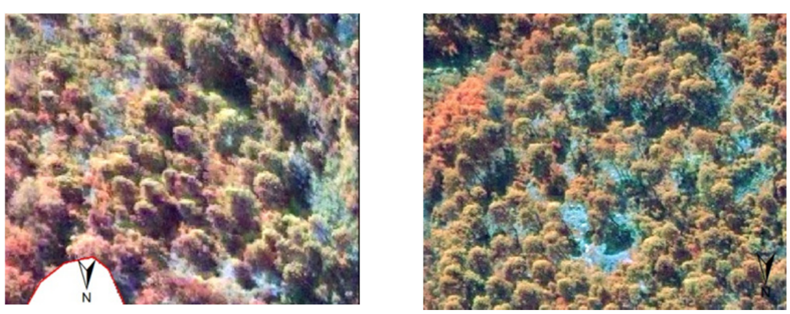

Figure 32. Screen shot of examples of irregular shaped tree crowns due to off-nadir view angle.

These irregular shapes of crowns could result in a disproportionate allometric relationship of CPA and other parameters such as biomass and carbon stock.

5.4.3. Effect of topography

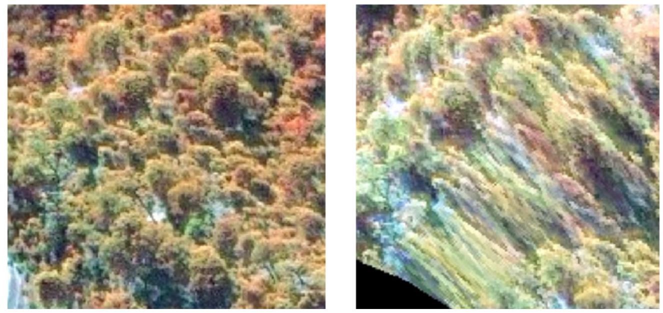

Figure 33. Screen shot showing the effect of ortho-rectification.

Before ortho-rectification on left side, after ortho-rectification on right side.

Effect of topography on tree crown delineation and crown allometric relationship with other parameters of trees has not been studied commonly. Pouliot (2005) discussed that topography also affects pixel size, which in turn can impact the crown size estimates and suggested that this effect could be minimized through ortho-rectification of a suitable digital elevation model. Even though, ortho-rectification of the image was suggested for the solution of topographic related issues on crown size estimates, in this research ortho-rectified image was causing abnormal distorted areas on the image (Figure 33). This distorted area occurred in small patches and its distribution was not systematic. For example, in some places where there is a very steep slope (up to 40^0), distorted part does not occur. Thus, very severely distorted parts were digitized and clipped out from the image analysis. Besides, rugged topography together with off-nadir view angle were influencing on projection of the crown differently. For example, in some parts the stems of trees were visible in the image while, it was not visible in some parts (Figure 32).

5.4.4. Other effects

As mentioned before, effect of understory and dense overlapping crowns can impact the delineated tree crowns. Moreover, errors related to field measurements such as measurement of tree stem diameter and height, sampling error and errors related to allometric equation may be propagated and influence the relationship between CPA and carbon stock of trees. Gonzalez *et al.* (2010) analysed the uncertainty of field measurement related errors and obtained high uncertainty on these measurements. In this research general allometric equation for broadleaf trees of moist tropical forest was used to calculate biomass and carbon stock since species specific allometric equations and general equation for broadleaf trees in mid-hills of Himalaya were not found through extensive literature search. This could introduce errors to the relationship of CPA and carbon stock of trees.

5.4.5. Magnitude of errors in analysis

Abovementioned source of errors can differently influence each analysis step of this research. Source of errors and their influence on each step is shown in Table 19.

Table 19**. Source of errors and their influence on different analysis steps in this research**

Source of errors	Tree crown delineation	Object based classification	Modelling CPA and carbon stock of tree
Shadow at tree crown level			X
Shadow at landscape level	X	X	X
Inclination angle			X
Topography			X
Understory and overlapping crowns	X	X	X
Field measurement and sampling error			X
Allometric equation			X

Exact estimation of magnitude of these errors of the study is beyond the scope of this research; however, understanding of it is crucial. From the source of errors, shadow at the landscape level and understory and overlapping tree crowns influenced to each step of analysis. While other sources of errors influence only modelling stage thus, finally resulting in lower R^2 on the relationship between CPA and carbon stock of trees.

Influence of inclination angle and topography cannot be shown on the accuracies of the tree crown delineation since the delineation of tree crowns was validated using reference tree crowns, which were digitized from the same image in this research.

5.5. Limitation of the research

The main limitations of this research were:

- High off-nadir view angle and less sun elevation of Geo-Eye image was the main limitation of this method. This is an important factor that determines the projection of the tree crown, especially when modelling has used image derived CPA.
- Processing capability of eCognition software limited the area used for the analysis, thus only subset area of Charnawati watershed was analysed and it resulted in fewer samples for the analysis.
- From the remotely sensed optical image, only top layer of the forest is visible in the image. In case of dense multi-layered forests and the presence of intermingled crowns, it is difficult to delineate tree crowns correctly.
- Reference tree crowns based on visual interpretation carry an error of subjectivity even though the crown diameter of some trees was used to reduce the subjectivity.

6. CONCLUSIONS AND RECOMMENDATIONS

6.1. Conclusion

The main objective of this study was to model carbon stock of trees using VHR Geo-Eye image and OBIA in case of central eastern part of Charnawati watershed, Dolakha district, Nepal. With respect to this, following conclusions were drawn for each research question.

What are the accuracies of tree crown delineation of ITC based approach Valley Following and eCognition based Region Growing approach?

In this research, the performances of two tree crown delineation approaches were compared. The result indicated that both the approaches provided useful results in delineating tree crowns in mixed forest. The Region Growing approach resulted in delineation accuracy of tree crown 30% error with 75% 1:1 correspondence while, Valley following approach delineated tree crowns having 40% error with 67% 1:1 correspondence.

Which tree crown delineation approach, Valley Following or Region Growing, is better?

As a result of T-test, it was concluded that Region Growing approach provides more accurate tree crown delineation than Valley Following approach in mixed forest. Analysis of the approaches indicated that each approaches has advantages and limitations.

What is the accuracy of tree species classification?

The accuracy of species classification at the tree crown level was 64.5% accuracy (Kappa=0.48) while more accurate classification was obtained from forest type classification (90.3% accuracy and Kappa=0.80). Use of separate classes in shaded area and non-shaded area improved the classification accuracy.

How strong is the relationship between the CPA and carbon stock of tree species

Weak relationship was found from the relationship of delineated CPA and carbon stock of broadleaf and needle leaf trees (R^2 of 0.16 and 0.34 respectively). Effects of shadow, sun elevation and off-nadir view angles of the image acquisition *etc.,* could have influenced to the relationship of CPA and carbon stock of trees.

This research indicated the utility of remote sensing based techniques, specifically VHR satellite imagery and OBIA in carbon stock estimation and other forest inventories.

6.2. Recommendation

VHR image and OBIA based automatic delineation and detection of tree crowns provides useful information about forest cover and its carbon content. This information can be further used for the projects of mitigating carbon dioxide in the atmosphere like REDD. More and more VHR sensors are being introduced in the world. This can make VHR images cost effective and can contribute to REDD project implementation in developing countries.

The effectiveness of tree crown delineation in mixed forest of Mid-hills of Nepal was tested in this research and this approach is recommended to be used in other natural mixed forests and plantation forests as well.

This research found that effect of shadow, sun elevation angle, off-nadir viewing angle were the main issues related to image and thus, use of image having a high sun elevation angle and low off-nadir viewing angle is recommended.

Moreover, it would be effective to use active remote sensing techniques to overcome issues of shadow effects, especially in this case of hilly terrain. LiDAR image can be a solution for shadow effects since it provides data regardless of the illumination condition and also height information of this can be applied for delineation of tree crowns. Despite the cost issue of LiDAR, combined use of high resolution optical imagery and LiDAR images is also suggested for effective delineation of tree crown and classification of them.

LIST OF REFERENCES

Aardt, J. A. N. v., Wynne, R. H., & Scrivani, J. A. (2008). Lidar-based Mapping of Forest Volume and Biomass by Taxonomic Group Using Structurally Homogenous Segments. *Photogrammetric Engineering & Remote Sensing, 74*, 11.

Ahmad, R., & Singh, R. P. (2002). Comparison of various data fusion for surface features extraction using IRS pan and LISS-III data. *Advances in Space Research, 29*(1), 73-78.

ANSAB. (2009). *Design and Setting up of a Governance and Payment Systems for Nepal's Community Forest Management Under Reducing Emission from Deforestation and Forest Degradation (REDD)*. Katmandu, Nepal.

Applegate, G. B., Gilmour, D. A., & Mohns, B. (1988). Biomass and productivity estimations for community forest management: a case study from the hills of Nepal -- I. Biomass and productivity of Chir Pine (Pinus roxburghii Sargent) plantations. *Biomass, 17*(2), 115-136.

Avsar, M. (2004). The relationships between diameter at breast height, tree height and crown diameter in Calabrian pines (Pinus brutia Ten.) of Baskonus Mountain, Kahramanmaras, Turkey. *J. Biol. Sci, 4*, 437-440.

Baccini, A., Friedl, M. A., Woodcock, C. E., & Warbington, R. (2004). Forest biomass estimation over regional scales using multisource data. *Geophysical Research Letters, 31*, 4 pp.

Bajracharya, D. M. (2010). Pytho-Geography of Nepal Himalaya. *Tribhuvan University Journal, 19*(2).

Basuki, T. M., van Laake, P. E., Skidmore, A. K., & Hussin, Y. A. (2009). Allometric equations for estimating the above-ground biomass in tropical lowland Dipterocarp forests. *Forest Ecology and Management, 257*(8), 1684-1694.

Blaschke, T. (2010). Object based image analysis for remote sensing. *ISPRS Journal of Photogrammetry and Remote Sensing, 65*(1), 2-16.

Brandtberg, T. (2002). Individual tree-based species classification in high spatial resolution aerial images of forests using fuzzy sets. *Fuzzy Sets and Systems, 132*(3), 371-387.

Brandtberg, T., & Walter, F. (1998). Automated delineation of individual tree crowns in high spatial resolution aerial images by multiple-scale analysis. *Machine Vision and Applications, 11*(2), 64-73.

Brown, S., Pearson, T., Slaymaker, D., Ambagis, S., Moore, N., Novelo, D., *et al.* (2005). Creating a virtual tropical forest from three-dimensional aerial imagery to estimate carbon stocks. *Ecological Applications, 15*(3), 1083-1095.

Bunting, P., & Lucas, R. (2006). The delineation of tree crowns in Australian mixed species forests using hyperspectral Compact Airborne Spectrographic Imager (CASI) data. *Remote Sensing of Environment, 101*(2), 230-248.

Chaturvedi, O., & Singh, J. (1982). Total biomass and biomass production of Pinus roxburghii trees growing in all aged natural forests. *Canadian Journal of Remote Sensing, 12*, 632-640.

Chave, J., Andalo, C., Brown, S., Cairns, M., Chambers, J., Eamus, D., *et al.* (2005). Tree allometry and improved estimation of carbon stocks and balance in tropical forests. *Oecologia, 145*(1), 87-99.

Chavez, P., Sides, S., & Anderson, J. (1991). Comparison of three different methods to merge multiresolution and multispectral data- Landsat TM and SPOT panchromatic. *Photogrammetric Engineering and Remote Sensing, 57*(3), 295-303.

Chubey, M. S., Franklin, S. E., & Wulder, M. A. (2006). Object-based analysis of ikonos-2 imagery for extraction of forest inventory parameters. *Photogrammetric Engineering and Remote Sensing, 72*, 383-394.

Clark, D. A., Brown, S., Kicklighter, D. W., Chambers, J. Q., Thomlinson, J. R., Ni, J., *et al.* (2001). Net primary production in tropical forests: An evaluation and synthesis of existing field data. *Ecological Applications, 11*, 371-384.

Clark, P. E., & Rilee, M. L. (2010). Processing Information and Data *Remote Sensing Tools for Exploration* (pp. 253-322): Springer New York.

Clinton, N., Holt, A., Scarborough, J., Yan, L., & Gong, P. (2010). Accuracy Assessment Measures for Object-based Image Segmentation Goodness. *Photogrammetric Engineering and Remote Sensing, 76*(3), 289-299.

Cochran, W. G. (1977). *Sampling techniques* (Third edition ed.). New York etc.: Wiley & Sons.

Coillie, F. M. B., Verbeke, L. P. C., & Wulf, R. R. (2008). Semi-automated forest stand delineation using wavelet based segmentation of very high resolution optical imagery. In T. Blaschke, S. Lang & G. J. Hay (Eds.), *Object-Based Image Analysis* (pp. 237-256): Springer Berlin Heidelberg.

Culvenor, D. S. (2002). TIDA: an algorithm for the delineation of tree crowns in high spatial resolution remotely sensed imagery. *Computers & Geosciences, 28*(1), 33-44.

Dahal, N., & Banskota, K. (2009). Cultivating REDD in Nepal's Community Forestry: A Discourse for Capitalizing on Potential? *Journal of Forest and Livelihood, 8*(1), 40-51.

Definiens. (2004). *eCognition User Guide 4: Concepts and Methods*. Munich, Germany: Definiens Imaging.

Definiens (2009). *eCognition Developer 8, reference book*. Munchen, Germany.

Dhital, N. (2009). Reducing Emissions from Deforestation and Forest Degradation (REDD) in Nepal: Exploring the Possibilities. *Journal of Forest and Livelihood, 8*(1), 55-62.

eCognition Community. (2008). Ruleset: Oil Palm Tree Delineation. Retrieved 15 November, 2010, from http://community.ecognition.com/home/0015_oil_palm_tree_delineation_364.zip/view?searchterm=oil+palm+tree

Erikson, M. (2003). Segmentation of individual tree crowns in colour aerial photographs using region growing supported by fuzzy rules. *Canadian Journal of Forest Research, 33*(8), 1557-1563.

Erikson, M. (2004). Species classification of individually segmented tree crowns in high-resolution aerial images using radiometric and morphologic image measures. *Remote Sensing of Environment, 91*(3-4), 469-477.

Erikson, M., & Olofsson, K. (2005). Comparison of three individual tree crown detection methods. *Machine Vision and Applications, 16*(4), 258-265.

Foli, E. G., Alder, D., Miller, H. G., & Swaine, M. D. (2003). Modelling growing space requirements for some tropical forest tree species. *Forest Ecology and Management, 173*(1-3), 79-88.

Foody, G. M., Boyd, D. S., & Cutler, M. E. J. (2003). Predictive relations of tropical forest biomass from Landsat TM data and their transferability between regions. *Remote Sensing of Environment, 85*(4), 463-474.

Gibbs, H. K. (2007). Monitoring and estimating tropical forest carbon stocks: making REDD a reality. *Environmental Research Letters, 2*(4), 045023.

Gonzalez, P., Asner, G. P., Battles, J. J., Lefsky, M. A., Waring, K. M., & Palace, M. (2010). Forest carbon densities and uncertainties from Lidar, QuickBird, and field measurements in California. *Remote Sensing of Environment, 114*(7), 1561-1575.

Gougeon, F. (1995). Crown-following approach to the automatic delineation of individual tree crowns in high spatial resolution aerial images. *Canadian Journal of Remote Sensing, 21*, 274-274.

Gougeon, F. (2010). *The ITC Suite Manual : A Semi-Automatic Individual Tree Crown (ITC) Approach to Forest Inventories*. Victoria, Canada: Canadian Forest Service.

Gougeon, F., & Leckie, D. G. (2006). The individual tree crown approach applied to Ikonos images of a coniferous plantation area. *Photogrammetric Engineering and Remote Sensing, 72*, 1287-1297.

Greenberg, J. A., Dobrowski, S. Z., & Ustin, S. L. (2005). Shadow allometry: Estimating tree structural parameters using hyperspatial image analysis. *Remote Sensing of Environment, 97*, 15-25.

Hay, G. J., Castilla, G., Wulder, M. A., & Ruiz, J. R. (2005). An automated object-based approach for the multiscale image segmentation of forest scenes. *International Journal of Applied Earth Observation and Geoinformation, 7*(4), 339-359.

Hemery, G., Savill, P., & Pryor, S. (2005). Applications of the crown diameter-stem diameter relationship for different species of broadleaved trees. *Forest Ecology and Management, 215*(1-3), 285-294.

Hijmans, R. J., Cameron, S., & Parra, J. (2005, 12 July 2006). WorldClim- Global Climate Data. Retrieved 17 August, 2010

Hirata, Y., Tsubota, Y., & Sakai, A. (2009). Allometric models of DBH and crown area derived from QuickBird panchromatic data in Cryptomeria japonica and Chamaecyparis obtusa stands. *International Journal of Remote Sensing, 30*(19), 5071-5088.

Hunt, C. A. G. (2009). *Carbon sinks and climate change : forests in the fight against global warming : e-book*. Cheltenham: Edward Elgar.

Husch, B., Beers, T. W., & Kershaw, J. A. (2003). *Forest mensuration* (Fourth edition ed.). Hoboken: Wiley & Sons.

ICIMOD, ANSAB, & FECOFUN. (2010). *Report on forest carbon stocks in Ludikhola, Kayarkhola and Charnawati Watersheds of Nepal*. Katmandu, Nepal.

IPCC. (2001) Summary for Policymakers. In: Climate Change 2001: The Physical Science Basis. Contribution of Working Group I to the Third Assessment Report of the Intergovernmental Panel on Climate Change Cambridge, United Kingdom and New York, NY, USA.: Cambridge University Press.

IPCC. (2006). IPCC Guidelines for National Greenhouse Gas Inventories, Chapter4 : Forest Land.

IPCC. (2007). *Summary for Policymakers. In: Climate Change 2007: The Physical Science Basis. Contribution of Working Group I to the Fourth Assessment Report of the Intergovernmental Panel on Climate Change [Solomon,* *S., D. Qin, M. Manning, Z. Chen, M. Marquis, K.B. Averyt, M.Tignor and H.L. Miller (eds.)].* Cambridge, United Kingdom and New York, NY, USA.

Jacquin, A., Misakova, L., & Gay, M. (2008). A hybrid object-based classification approach for mapping urban sprawl in periurban environment. *Landscape and Urban Planning, 84*(2), 152-165.

Junli, L., Jiabing, S., & Xi, M. (2005). Multiresolution fusion of remote sensing images based on resolution degradation model. *Geo-Spatial Information Science, 8*(1), 50-56.

Jyoti Nath, A., Das, G., & Das, A. K. (2009). Above ground standing biomass and carbon storage in village bamboos in North East India. *Biomass and Bioenergy, 33*(9), 1188-1196.

Kajisa, T., Murakami, T., Mizoue, N., Top, N., & Yoshida, S. (2009). Object-based forest biomass estimation using Landsat ETM plus in Kampong Thom Province, Cambodia. *Journal of Forest Research, 14*(4), 203-211.

Kasischke, E. S., Melack, J. M., & Dobson, M. C. (1997). Use of imaging radars for ecological applications - a review. *Remote Sensing of Environment, 59*, 141-156.

Katoh, M., Gougeon, F. A., & Leckie, D. G. (2009). Application of high-resolution airborne data using individual tree crowns in Japanese conifer plantations. *Journal of Forest Research, 14*, 10-19.

Ke, Y., & Quackenbush, L. (2008). *Comparison of individual tree crown detection and delineation methods.* Paper presented at the ASPRS Annual conference "Bridging the Horizons: New Frontiers in Geospatial Collaboration", Portland, Oregon, US.

Ke, Y., Quackenbush, L. J., & Im, J. (2010). Synergistic use of QuickBird multispectral imagery and LIDAR data for object-based forest species classification. *Remote Sensing of Environment, 114*(6), 1141-1154.

Kim, M., Madden, M., & Warner, T. A. (2009). Forest Type Mapping using Object-specific Texture Measures from Multispectral Ikonos Imagery: Segmentation Quality and Image Classification Issues. [Article]. *Photogrammetric Engineering and Remote Sensing, 75*(7), 819-829.

Köhl, M., Magnussen, S., & Marchetti, M. (2006). Sampling in Forest Surveys *Sampling Methods, Remote Sensing and GIS Multiresource Forest Inventory* (pp. 71-196): Springer Berlin Heidelberg.

Kuuluvainen, T. (1991). Relationships between crown projected area and components of above-ground biomass in Norway spruce trees in even-aged stands: Empirical results and their interpretation. *Forest Ecology and Management, 40*(3-4), 243-260.

Le Toan, T., Quegan, S., Woodward, I., Lomas, M., Delbart, N., & Picard, G. (2004). Relating radar remote sensing of biomass to modelling of forest carbon budgets. [Proceedings Paper]. *Climatic Change, 67*(2-3), 379-402.

Leboeuf, A., Beaudoin, A., Fournier, R. A., Guindon, L., Luther, J. E., & Lambert, M. C. (2007). A shadow fraction method for mapping biomass of northern boreal black spruce forests using QuickBird imagery. *Remote Sensing of Environment, 110*(4), 488-500.

Leckie, D., Jay, C., Gougeon, F., Sturrock, R., & Paradine, D. (2004). Detection and assessment of trees with Phellinus weirii (laminated root rot) using high resolution multi-spectral imagery. *International Journal of Remote Sensing, 25*(4), 793-818.

Leckie, D. G., Gougeon, F. A., Tinis, S., Nelson, T., Burnett, C. N., & Paradine, D. (2005). Automated tree recognition in old growth conifer stands with high resolution digital imagery. *Remote Sensing of Environment, 94*(3), 311-326.

Leckie, D. G., Gougeon, F. A., Walsworth, N., & Paradine, D. (2003). Stand delineation and composition estimation using semi-automated individual tree crown analysis. *Remote Sensing of Environment, 85*(3), 355-369.

Lu, D. (2005). Aboveground biomass estimation using Landsat TM data in the Brazilian Amazon. *International Journal of Remote Sensing, 26*, 2509-2525.

Lu, D. (2006). The potential and challenge of remote sensing-based biomass estimation. *International Journal of Remote Sensing, 27*(7), 1297-1328.

Malhi, Y., & Grace, J. (2000). Tropical forests and atmospheric carbon dioxide. [doi: DOI: 10.1016/S0169-5347(00)01906-6]. *Trends in Ecology & Evolution, 15*(8), 332-337.

Martin, A., Laanaya, H., & Arnold-Bos, A. (2006). Evaluation for uncertain image classification and segmentation. *Pattern Recognition, 39*(11), 1987-1995.

Mohns, G. (1988). Biomass and productivity estimations for community forest management: A case study from the hills of Nepal--II. Dry matter production in mixed young stands of chir pine (Pinus roxburghii) and broad-leaved species. *Biomass, 17*(3), 165-184.

Möller, M., Lymburner, L., & Volk, M. (2007). The comparison index: A tool for assessing the accuracy of image segmentation. *International Journal of Applied Earth Observation and Geoinformation, 9*(3), 311-321.

Mora, B., Wulder, M. A., & White, J. C. (2010). Segment-constrained regression tree estimation of forest stand height from very high spatial resolution panchromatic imagery over a boreal environment. *Remote Sensing of Environment, In Press, Corrected Proof.*

Morales, R., Miura, T., & Idol, T. (2008). An assessment of Hawaiian dry forest condition with fine resolution remote sensing. *Forest Ecology and Management, 255*(7), 2524-2532.

Neteler, M., & Mitasova, H. (2004). Satellite Image Processing *Open Source GIS: A Grass GIS Approach* (Vol. 773, pp. 201-252): Springer US.

Neteler, M., & Mitasova, H. (2008). Open Source GIS. In M. Neteler & H. Mitasova (Eds.), (pp. 287-329): Springer US.

Olofsson, K. (2002). *Detection of single trees in aerial images using template matching.* Paper presented at the ForestSAT Symposium Heriot Watt University,, Edinburgh, UK.

Olofsson, K., Wallerman, J., Holmgren, J., & Olsson, H. (2006). Tree species discrimination using Z/I DMC imagery and template matching of single trees. *Scandinavian Journal of Forest Research, 21*, 106-110.

Ozdemir, I. (2008). Estimating stem volume by tree crown area and tree shadow area extracted from pan-sharpened Quickbird imagery in open Crimean juniper forests. *International Journal of Remote Sensing, 29*(Copyright 2008, The Institution of Engineering and Technology), 5643-5655.

Palace, M., Keller, M., Asner, G. P., Hagen, S., & Braswell, B. (2008). Amazon Forest Structure from IKONOS Satellite Data and the Automated Characterization of Forest Canopy Properties. *Biotropica, 40*(2), 141-150.

Pande, H., Tiwari, P. S., & Dobhal, S. (2009). Analyzing hyper-spectral and multi-spectral data fusion in spectral domain. *Journal of the Indian Society of Remote Sensing, 37*(3), 395-408.

Panta, M., Kim, K., & Joshi, C. (2008). Temporal mapping of deforestation and forest degradation in Nepal: Applications to forest conservation. *Forest Ecology and Management, 256*(9), 1587-1595.

Platt, R. V., & Schoennagel, T. (2009). An object-oriented approach to assessing changes in tree cover in the Colorado Front Range 1938-1999. *Forest Ecology and Management, 258*(7), 1342-1349.

Pollock, R., & Woodham, R. (1996). *The automatic recognition of individual trees in aerial images of forests based on a synthetic tree crown image model*: National Library of Canada= Bibliothèque nationale du Canada.

Pouliot, D., King, D., Bell, F., & Pitt, D. (2002). Automated tree crown detection and delineation in high-resolution digital camera imagery of coniferous forest regeneration. *Remote Sensing of Environment, 82*(2-3), 322-334.

Pouliot, D., King, D., & Pitt, D. (2005). Development and evaluation of an automated tree detection–delineation algorithm for monitoring regenerating coniferous forests. *Canadian Journal of Forest Research, 35*(10), 2332-2345.

Rohner, M., & Staub, M. (2008). *Embracing the challenges of Climate Change.* Paper presented at the Geneva International Model United Nations.

Sharma, R. (1999). Modelling growing space requirement for Alnus nepalensis D. Don in Nepal. *E-mail: bankojanakari@ gmail. com*, 30.

Shimano, K. (1997). Analysis of the relationship between DBH and crown projection area using a new model. *Journal of Forest Research, 2*(4), 237-242.

Shrestha, P. M., & Dhillion, S. S. (2003). Medicinal plant diversity and use in the highlands of Dolakha district, Nepal. *Journal of Ethnopharmacology, 86*(1), 81-96.

Song, C., Dickinson, M. B., Su, L., Zhang, S., & Yaussey, D. (2010). Estimating average tree crown size using spatial information from Ikonos and QuickBird images: Across-sensor and across-site comparisons. *Remote Sensing of Environment, 114*(5), 1099-1107.

Steininger, M. K. (2000). Satellite estimation of tropical secondary forest above-ground biomass: data from Brazil and Bolivia. *International Journal of Remote Sensing, 21*(6-7), 1139-1157.

Thompson, S. K. (2002). *Sampling* (Second edition ed.). Chichester etc.: Wiley & Sons.

Tiede, D., Lang, S., & Hoffmann, C. (2008). Domain-specific class modelling for one-level representation of single trees. In T. Blaschke, S. Lang & G. J. Hay (Eds.), *Object-Based Image Analysis* (pp. 133-151): Springer Berlin Heidelberg.

UN-REDD. (2008). *UN Collaborative Programme on Reducing Emissions from Deforestation and Forest Degradation in Developing Countries (UN-REDD) :Framework Document.*

Verwijst, T., & Telenius, B. (1999). Biomass estimation procedures in short rotation forestry. *Forest Ecology and Management, 121*(1-2), 137-146.

Wang, L., Gong, P., & S.Biging, G. (2004). Individual Tree-Crown Delineation and Treetop Detection in High Spatial Resolution Areal Imagery. *Photogrammetric Engineering and Remote Sensing, 70*(3), 351-357.

Wulder, M., Niemann, K., & Goodenough, D. (2000). Local maximum filtering for the extraction of tree locations and basal area from high spatial resolution imagery. *Remote Sensing of Environment, 73*(1), 103-114.

Z Li, R Hayward, J Zhang, Y Liu, & Walker, R. (2009). *Towards Automatic Tree Crown Detection and Delineation in Spectral Feature Space Using PCNN and Morphological Reconstruction.* Paper presented at the *IEEE 16th International Conference on Image Processing ICIP 2009*, Cairo, Egypt.

Zhan, Q. M., Molenaar, M., Tempfli, K., & Shi, W. Z. (2005). Quality assessment for geo-spatial objects derived from remotely sensed data. [Proceedings Paper]. *International Journal of Remote Sensing, 26*(14), 2953-2974.

Zhang, W., Ke, Y., Quackenbush, L., & Zhang, L. (2010). Using error-in-variable regression to predict tree diameter and crown width from remotely sensed imagery. *Canadian Journal of Forest Research, 40*(6), 1095-1108.

Zianis, D., & Mencuccini, M. (2004). On simplifying allometric analyses of forest biomass. *Forest Ecology and Management, 187*(2-3), 311-332.

APPENDICES

Appendix 1. Locations of total collected sample plots

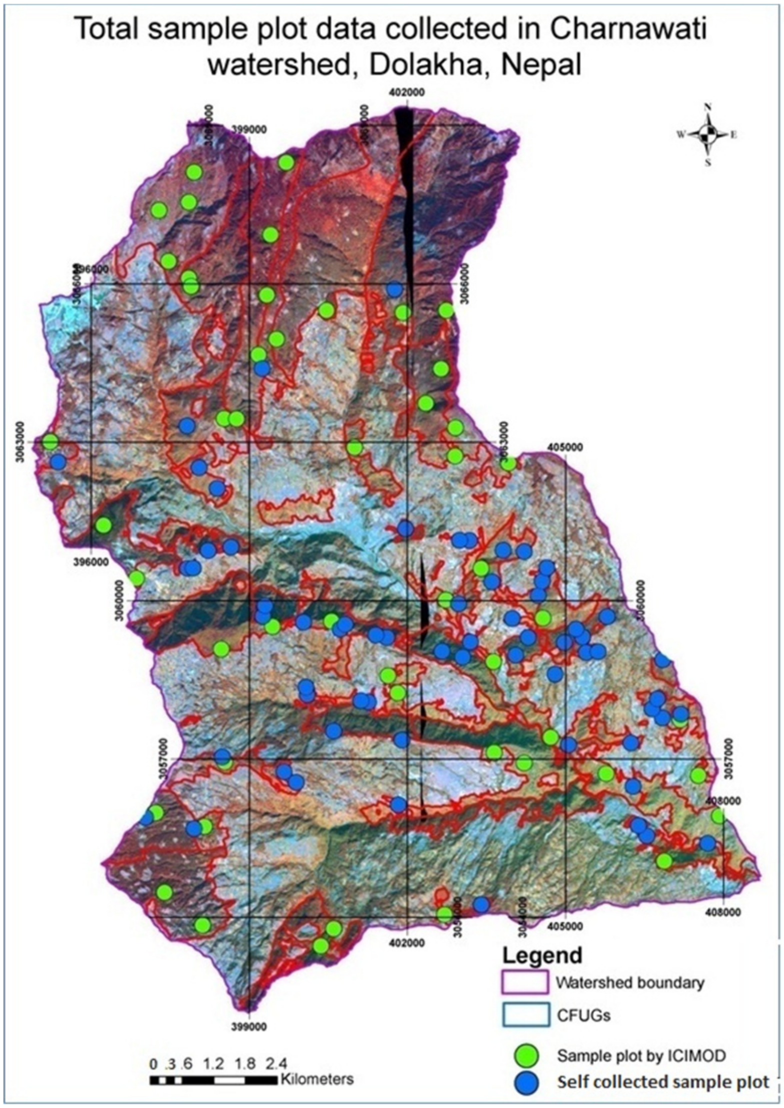

Appendix 2. Recording sheet used in the field

<table>
<tr><td colspan="3">Name of the recorder:</td><td colspan="5">Date:</td></tr>
<tr><td colspan="3">Map Scale:</td><td colspan="5">Map No.:</td></tr>
<tr><td rowspan="2">Sampling Plot No.</td><td colspan="2">Grid ref. Land Mark</td><td rowspan="2">Dist. To centre of plot</td><td rowspan="2">Bearing to centre of plot</td><td rowspan="2">Elevation</td><td rowspan="2">Slope (%)</td><td rowspan="2">Aspect</td></tr>
<tr><td>X</td><td>Y</td></tr>
<tr><td></td><td></td><td></td><td></td><td></td><td></td><td></td><td></td></tr>
</table>

<table>
<tr><td colspan="12">Forest characteristics</td></tr>
<tr><td colspan="3">Land cover</td><td colspan="5">Forest use type</td><td>Crown cover (%)</td><td>Stand composition</td><td>Type of Stand</td><td>Undergrowth</td></tr>
<tr><td>F</td><td>N</td><td>G</td><td>M</td><td>P</td><td>N</td><td>R</td><td>Pr</td><td></td><td rowspan="2"></td><td rowspan="2"></td><td rowspan="2"></td></tr>
<tr><td></td><td></td><td></td><td></td><td></td><td></td><td></td><td></td><td></td></tr>
</table>

Tree No.	Species	DBH (cm)	Height (m)	Crown diam (n)	Tree class				
1					1	2	3	4	d
2									
3									
.									
.									
.									
30									
Remarks:									
Legend/ Abbreviations									
Landcover - F- Forest, N-Non-Forest, G- Grassland			***Forest use type*** - M- Managed forest, P- Protection Forest, N- Natural Reserve, Pr- Production forest, R- Recreation						

Tree No.	**Species**	**DBH (cm)**	**Height (m)**	**Crown diam (n)**	**Tree class**				
A					1	2	3	4	d
B									
C									
.									
.									
.									
N									

Appendix 3. List of local tree species

	Local name	**Scientific name**
1	Aakhatura	
2	Aarupate	*Prunus cornuta*
3	Amala	*Emblica efficinalis*
4	Amala	*Phyllanthus emblica*
5	Amsi	
6	Angeri	*Lyonia ovalifolia*
7	Arupatti	*Prunus napaulensis*
8	Baanjh	*Quercus incana 2*
9	Badkule	
10	Balkal Pate	*Symplocos theaefelia*
11	Bhalayo	*Rus succedanea*
12	Chhotro	*Berberis asiatica*
13	Chilaune	*Schima Wallichiana*
14	Dhudilo	*Hedera helix*
15	Falant	*Quercus glauca*
16	Ghingane	*Euriya accuminata*
17	Ghingane	*Euriya cerasifolia*
18	Ghurmiso	
19	Gineri	*Pieris formosa*
20	Gobliso	
21	Gobre Salla	*Abies spectabilis*
22	Guenli	*Elaeagnus latifolia*
23	Guras	*Rhododendron arboreum*

24	Jamuna	*Syzygium cumini*
25	Kafal	*Myrica esculenta*
26	Kainyo	*Gravelia robusta*
27	Kalikath	*Myrsine semiserrata*
28	Khamali	*Ficus roxburghii*
29	Kharane	*Sympleces ramesissima*
30	Kharsu	*Quercus semicarpifolia*
31	Khirro	*Sapium insigne*
32	Kholme	*Symplocos pyrifolia*
33	Khorsani	*Capsicum annuum*
34	Khote Salla	*Pinus roxburghii*
35	Kutmero	*Litsea polyantha*
36	Kwanle	
37	Lankuri	*Fraxinus floribunda*
38	Lapsi	*Choerospondias axillaris*
39	Mahalo	*Viburnum cerdifelium*
40	Male	*Pyrus pashia*
41	Masala	*Eucalyptus sp.*
42	Mauwa	*Engelhardicta spicata*
43	Nilo chimal	*Rhododendendron campanulatum*
44	Omsisi	
45	Paati	*Eurya japonica*
46	Pahele	*Benthamedia capitata*
47	Pate Salla	*Pinus patula*
48	Patpate	*Leycesterin formosa*
49	Pipire	*Bucklandia*
50	Priya ghans	*Persicaria nepalensis*
51	Prunus	*Prunus ceracoides*
52	Ragchan	*Daphniphyllum himalense*
53	Raktachandan	*Pterocarpus santalinus*
54	Rani Salla	*Pinus wallichiana*
55	Rato kangio	*Wedlandia coreacea*
56	Sal	*Shorea Robusta*
57	Sauer	*Betula alnoides*
58	Setikath	*Myrsine capitellata*
59	Shilinge	
60	Sissoo	*Dalbergia sissoo*
61	Thingre salla	*Tsugadomusa*
62	Thulo bhalayo	*Rhus wallichii*
63	Thulo dhaire	
64	Uttis	*Alnus nepalensis*

Appendix 4. Comparison of spectral mean and maximum value of tree crown of different species using a line chart

a. Spectral mean value of tree crown of different species; b. Spectral maximum value of tree crown of different species

a.

b.

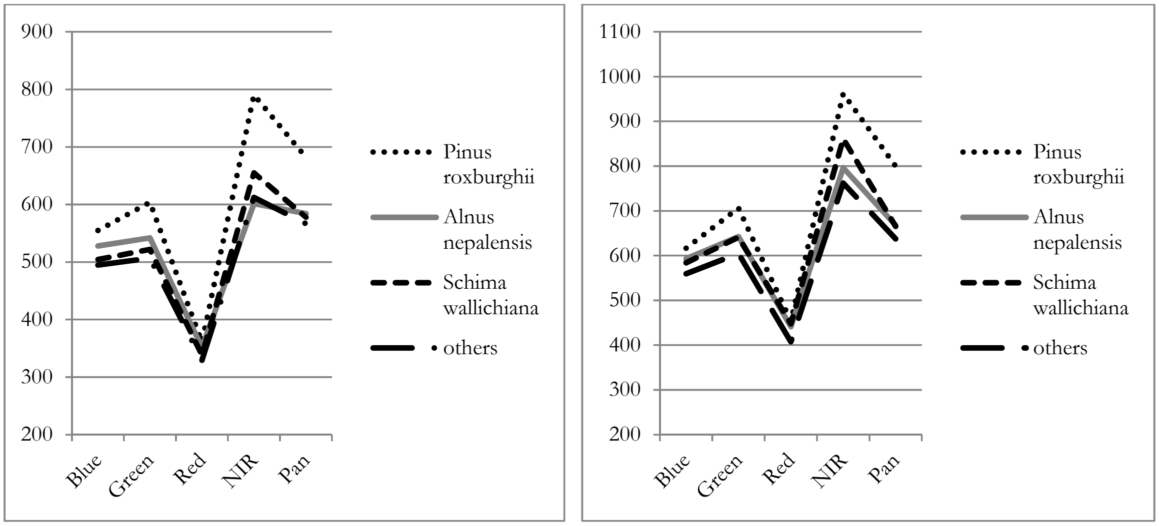

Appendix 5. Correlation of CPA and Carbon stock of trees in shaded and non-shaded areas

		Needle leaf			Broadleaf		
		Shaded	Non shaded	Total	Shaded	Non Shaded	total
	Count	**6**	**39**	**45**	**36**	**24**	**60**
Correlation	Reference CPA	0.83	0.73	0.73	0.19	0.73	0.49
	Delineated CPA	0.60	0.53	0.52	0.15	0.65	0.40

Appendix 6. Photos from the field








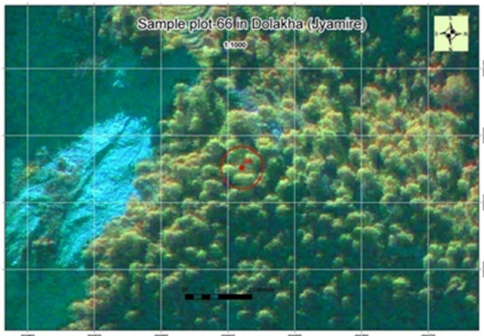
Sample plot-66 in Dolakha (Jyamire)
1:1000


Sample plot-45 in Dolakha (Mahankal)